MOLECULAR MOBILITY IN SUGAR GLASSES

Promotor: dr. E. van der Linden, hoogleraar in fysica en fysische chemie van levensmiddelen

Copromotor: dr. M.A. Hemminga, universitair hoofddocent, departement biomoleculaire wetenschappen

MOLECULAR MOBILITY IN SUGAR GLASSES

Ivon J. van den Dries

Proefschrift

ter verkrijging van de graad van doctor

op gezag van de rector magnificus

van Wageningen Universiteit

dr. C.M. Karssen,

in het openbaar te verdedigen

op 17 mei 2000

des namiddags te 16.00 in de aula

Stellingen

1. De *toenemende* beweeglijkheid van de watermoleculen als ook de *afnemende* beweeglijkheid van spin probe moleculen in suikerglazen met toenemend watergehalte zijn beide een gevolg van veranderingen in de moleculaire pakking.
   (dit proefschrift, hoofdstuk 4)

2. De oorsprong van collapse verschijnselen in suikerglazen is een *plotselinge* toename in de beweeglijkheid van de suikermoleculen.
   (dit proefschrift, hoofdstuk 5)

3. Het feit dat de korte termijn stabiliteit van suikerglazen niet gerelateerd is aan de glasovergangstemperatuur maar aan de collapse temperatuur komt doordat pas bij de collapse temperatuur een grote verandering in de moleculaire beweging optreedt.
   (dit proefschrift, hoofdstuk 5)

4. De afnemende aandacht voor het geloof en de toenemende aandacht voor materiële zaken uit zich onder andere in het feit dat bankgebouwen tegenwoordig hoger de hemel in reiken dan kerken.

5. Het feit dat Ada Yonath na 30 jaar aan de röntgenstructuur van het ribosoom te hebben gewerkt in 4 jaar werd voorbij gestreefd door Tom Steitz toont aan dat goede timing esentiëler is dan toewijding voor succes in de wetenschap.

6. Het sneller worden van telecommunicatie en computers en de daarmee gepaard gaande tijdsbesparing heeft er niet toe geleid dat men meer tijd over heeft.

7. De structuur van onze wereld is afhankelijk van de structuur van ons lichaam.
   (gebaseerd op 'phenomenoloy of perception' van M. Merleau-Ponty)

8. Bossen aanplanten in derde wereldlanden ter compensatie van de CO_2 uitstoot in Europa is een vorm van neokolonialisme.

Ivon van den Dries
Molecular mobility in sugar glasses
Wageningen, 17 mei 2000

CONTENTS

1

Introduction

A glass is a liquid with solid state like behavior as a result of its extremely high viscosity [1-3]. The occurrence of a glass transition is an almost universal property of liquids [1]. A well-known example is silicium oxide glass, commonly called 'glass'. Another applicability of glasses is the use of polymer glasses as plastics. The glass transition in these plastics denotes the transition from a brittle glass to a rubber. A few examples of partially glassy or glassy foods are candies, crackers, crisps, milk and coffee powder, cookies, ice cream and cereals.

The glassy state of foods and food materials is studied because the glass transition plays a role in the preservation of foods [4]. As a model system for low moisture and frozen foods, we study sugar glasses since sugars in low moisture or frozen foods often exist in the glassy state. Most low moisture and frozen foods are not stable and exhibit time-dependent changes in quality as a result of phenomena such as phase separation, crystallization of component compounds, chemical and enzymatic reactions, flavor loss and changes in texture [5]. Many of these changes are kinetically controlled by the glass transition temperature [6, 7]. Key factors controlling the stability of glassy materials are water content, time and temperature [6, 7]. For example moisture uptake will decrease the glass transition temperature of a sugar glass below storage temperature and the sugars will tend to crystallize.

Much research related to the stability of amorphous sugar systems has been performed on amorphous solid dosage forms of drugs [8-12]. Amorphous dosage forms are preferred above crystalline dosage forms because of their better solubility and accelerated dissolution properties, however a disadvantage is their instability [8]. The same factors controlling the stability of amorphous foods apply to the stability of pharmaceuticals with that difference that pharmaceuticals are in general stored for longer periods of time than foods.

2

A common statement is that the amorphous state is stable below its glass transition temperature due to restricted molecular mobility [6, 7]. In terms of molecular mobility, glass formation is explained as follows: If, upon cooling, a liquid does not crystallize at its melting point, and is cooled down further, it is called a supercooled liquid. As a supercooled liquid is cooled to lower temperatures its viscosity increases and the movement of the liquid molecules decreases. At some temperature the molecular movement will be so slow that the molecules do not have the chance to reorient themselves significantly before the temperature is lowered further. The timescale of motion becomes so long that the motion is frozen on the timescale of experimental observation and this is the glass transition temperature [2]. However, when the molecular mobility is frozen on the timescale of experimental observation, this is no guarantee for stability on the timescale of storage of products [8-10, 13]. The question what the best storage conditions are to stabilize pharmaceutical dosage forms has been formulated as follows [9]: "Under what conditions (e.g. temperature, humidity) do the molecular processes responsible for destabilization of an amorphous substance become precluded or statically improbable over the normal life-time of a pharmaceutical product? ". All destabilizing processes in low moisture and frozen foods, as mentioned above are related to molecular mobility. For example the use of amorphous sugars as encapsulation matrices for flavors depends on the ability to retard the molecular motion of the flavor molecules.

The aim of this thesis is to relate molecular mobility around the glass transition to the effects of physical parameters like water content and temperature on the stability of sugar-water mixtures. This molecular mobility in sugar-water mixtures is studied by means of magnetic resonance techniques. The molecular mobility of water and sugar protons is measured directly with proton nuclear magnetic resonance (^{1}H-NMR) techniques. In addition, indirect

information on molecular mobility in sugar water glasses is obtained using electron spin resonance (ESR) techniques, monitoring the mobility of a spin probe. In order to relate molecular mobility to the effects of temperature and water content on the stability of sugar water systems, one needs a characterization of the various states the system can be in. This characterization is summarized in a state diagram. It describes the various states of a sugar solution as a function of water content and temperature including the liquid and crystal phases, but also thermodynamically unstable states such as glasses (See Fig. 1-1 state diagram of glucose)[14, 15]. The glass transition temperature as a function of water content is denoted by line AB in Fig. 1-1 where A is the glass transition temperature of pure water and B the glass transition temperature of pure glucose [16]. The line AB is found by mixing the right amount of glucose and water, melting this mixture and cooling it to low temperatures, fast enough to prevent crystallization. Upon warming, the glass
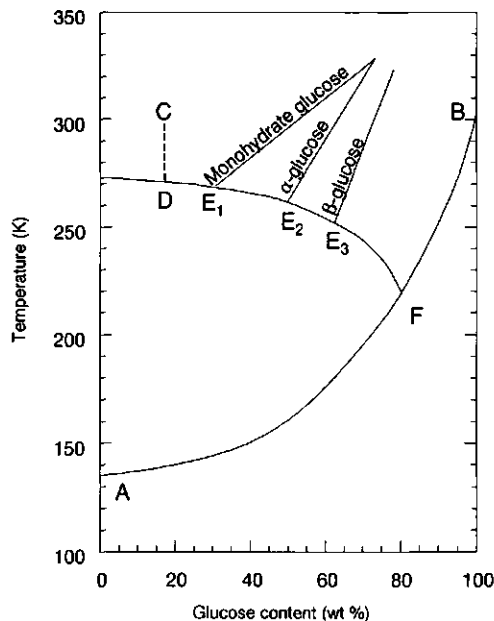

Figure 1 State diagram of glucose. Solubility data are taken from Young [14] and the glass transition data from Noel et al. [16].

4

transition temperature of the mixture determines the point of line AB at the glucose concentration of the mixture [16]. Line DE_3 is the freezing point depression line of the aqueous glucose solution, as determined for glucose by Young [14]. For example, if a 20 wt % glucose solution is cooled (line CD in Fig. 1-1) ice start to form at 270 K thus leading to a two phase system at point D. Subsequent cooling yields more ice formation and thus a more concentrated glucose solution. Thus, in a concentrated glucose solution ice formation takes place at a lower temperature, leading to a continuously declining freezing point depression line. At point E_1 the solubility limit is reached for the glucose-water phase and monohydrate glucose crystals should be formed. In practice glucose will mutarotate to form β-glucose and glucose-monohydrate and α-glucose will not crystallize at point E_1 and E_2 [14]. Subsequent freezeconcentrating to a 60 wt % glucose (point E_3 in Fig. 1-1), the solubility limit of β-glucose is reached and crystallization should occur. This crystallization process is divided into a nucleation process and a crystal growth process, and, if one of these two processes is hindered, crystallization is avoided. Glucose solutions can easily be freezeconcentrated further than 60 wt% without sugar crystallization and following line E_3F in Fig. 1-1 a maximally freezeconcentrated glass is formed at point F, where the freezing point depression line crosses the glass transition line. It is noted that line EF represents a non-equilibrium line and reflects the history of the sample. For example the cooling rate determines the amount of ice formed and the concentration of glucose. Thus the cooling rate determines the exact position of point F. A maximally freezeconcentrated sample consist of 81 wt% glucose [5]. Both concentrated sugar-water glasses prepared from the melt and freezeconcentrated sugars are studied in this thesis.

In relating molecular mobility to the effects of temperature and water content on stability of sugar water systems, one needs to define the term molecular mobility more accurately. In fact, three types of molecular motion can be

5

distinguished: vibrational, rotational and translational motion. The first type, vibrational motions, are sensitive for inter- and intramolecular interactions and can be studied by Fourier Transform Infrared Spectroscopy (FTIR). A sugar molecule has many vibrational transitions. However, many can be assigned to particular bonds. The band position in a FTIR spectrum depends on the intrinsic molecular vibration and its microenvironment. For example, the OH stretching vibration is sensitive for the glass transition in sugar-water mixtures [17]. The translational motion of the sugar molecules is too slow to be measured in glasses. The translational water mobility can be directly studied by drying the sugar-water glasses and following the decrease in weight [18-20] or by pulsed field gradient Nuclear Magnetic Resonance (NMR)[21].

The rotational mobility of both water and sugar can be directly studied by dielectric measurements[16, 22], or a variety of NMR techniques [12, 23-30]. We study the ^{1}H-NMR signal after a 90° pulse, which originates from two fractions of protons, solid protons and mobile protons ($\tau_R < 3*10^{-6}$ s). The mobile protons, mainly water protons, are characterized by a spin-spin relaxation time T_{2m}, which is correlated with rotational mobility. The solid protons are characterized by the second moment (M_2), which is a measure of unaveraged dipolar couplings. The second moment is sensitive for slow isotropic mobility ($\tau_R > 3 * 10^{-6}$ s) and anisotropic mobility such as side group motion and internal molecular motion.

Implicit information regarding the mobility of water and sugar molecules can be obtained by monitoring the rotational and translational motion of a probe molecule added to the sugar-water mixture [31-38]. The mobility of the probe molecules in sugar water glasses can be followed over a broad range of mobilities using optical techniques such as Fluorescence Recovery After Photobleaching (FRAP) [34, 36] or spin probe Electron Spin Resonance (ESR)

techniques [38], provided that the probe has fluorescent groups or stable free radicals, respectively. The advantage of ESR spin probe techniques is that non-transparent samples can be studied, which are not assessable with optical techniques. The advantage of FRAP is that both rotational as well as translational probe mobility can be studied. Conventional ESR is sensitive to rotational correlation times (τ_R) between 10^{-11} and 10^{-8} s. However, because of the high viscosity of sugar solutions around their glass transition temperature a ESR technique was needed which has access to lower mobilities. In the region of $\tau_R > 10^{-6}$ s, Saturation Transfer ESR (STESR) is used[39-43]. A new data analysis method for ST-ESR spectra, which is described in chapter 2, made it possible to measure τ_R values in the range from 10^{-6} s $< \tau_R < 10^{+4}$ s. In order to compare the direct with the indirect approach, proton mobility of the sugar and water molecules as obtained with ^{1}H-NMR techniques is compared with rotational mobility of a spin probe obtained with ESR techniques.

The first part of this thesis (chapters 2 and 3) addresses the use of the magnetic resonance techniques to study the mobility in glasses. In chapter 2 it is described how the limit of sensitivity for mobility of the ST-ESR technique is extended by a new data analysis technique. This extension was necessary in order to get access to the very slow spin probe mobility in glasses. In chapter 3, it is discussed how the water and sugar mobility can be studied by ^{1}H-NMR techniques. In the ^{1}H-NMR signal slow and fast decaying protons are distinguished as arising from mobile and immobile protons, respectively. In order to study water and sugar mobility the mobile and immobile protons have to be assigned to water and sugar protons. Via the relaxation behavior of both fractions information about their mobility could be obtained.

The second part of this thesis (chapters 4 and 5) addresses the relation between molecular mobility and physical parameters that characterize the stability of glasses. In chapter 4, both NMR and ESR techniques are applied to

study water and spin probe mobility in glucose and maltose as a function of water content and temperature. The results are complemented by additional structural information about the hydrogen-bonded network, as obtained with FTIR. Furthermore, the spin probe mobility is studied as a function of molecular weight of malto oligomers, with 1 to 7 glucose units. The structural information about the hydrogen bonded network and the molecular mobility results are combined, and effects of water content and molecular weight of the malto oligomers are explained in terms of molecular packing. Chapter 5 describes study of the immobile protons in glucose-water mixtures. This study reveals a second transition in mobility, occurring above T_g, which can be related to macroscopic collapse phenomena.

REFERENCES

1. M. Goldstein. *J. Chem. Phys.* **1969**, *51*, 3728.

2. M. D. Ediger, C. A. Angell and S. R. Nagel. *J. Phys. Chem.* **1996**, *100*, 13200-13212.

3. C. A. Angell. *J. Phys. Chem of Solids* **1988**, *49*, 863-871.

4. H. Levine and L. Slade. *Cryo-Lett.* **1988**, *9*, 21-63.

5. Y. Roos *Phase Transitions in Foods*; Academic Press: San Diego, 1995.

6. L. Slade and H. Levine. *Food science and Nutrition* **1991**, *30*, 115.

7. L. Slade and H. Levine. The glassy state phenomenon in food molecules. In *The glassy state in foods*; J. M. V. Blanshard and P. J. Lillford, Eds.; Nottingham University Press: Nottingham, 1993; pp 35-102.

8. D. Q. M. Craig, P. G. Royall, V. L. Kett and M. L. Hopton. *Int. J. Pharm.* **1999**, *179*, 179-207.

9. B. C. Hancock, S. L. Shamblin and G. Zografi. **1995**, *Pharm. Res*, 12(6), 799-806.

10. B. C. Hancock and G. Zografi. *J. Pharm. Sci.* **1997**, *86*, 1-12.

11. G. Zografi and S. R. Byrn. the effects of residual water on solid-state stability of drugs and drug products. In *Water management in the design and distribution of quality foods*; Y. H. Roos, R. B. Leslie and P. J. Lillford, Eds.; Technomic: Lancaster, 1999; pp 397-410.

12. C. A. Oksanen and G. Zografi. *Pharm. Res.* **1993**, *10*, 791-9.

13. S. L. Shamblin, X. Tang, L. Chang, B. C. Hancock and M. J. Pikal. *J. Phys. Chem. B* **1999**, *103*, 4113-4121.

14. F. E. Young. *J. Phys. Chem.* **1957**, *61*, 616.

15. B. Luyet and D. Rasmussen. *Biodynamica* **1968**, *10*, 167-191.

16. T. R. Noel, R. Parker and S. G. Ring. *Carbohydr. Res.* **1996**, *282*, 193-206.

17. W. F. Wolkers, H. Oldenhof, M. Alberda and F. A. Hoekstra. *Biochim. Biophys. Acta* **1998**, *1379*, 83-96.

18. B. J. Aldous, F. Franks and A. L. Greer. *J. Mat. Sc.* **1997**, *32*, 301-308.

19. R. Parker and S. G. Ring. *Carbohydr. Res.* **1995**, *273*, 147-55.

20. R. H. Tromp, R. Parker and S. G. Ring. *Carbohydr. Res.* **1997**, *303*, 199-205.

21. D. Girlich, H. D. Lüdemann, C. Buttersack and K. Buchholz. *Z. Naturforsch. C* **1994**, *49*, 696.

22. R. K. Chan, K. Pathmnathan and G. P. Johari. *J. Phys. Chem.* **1986**, *90*, 6358-6362.

23. D. Girlich and H.-D. Lüdemann. *Z. Naturforsch.* **1993**, *49*, 250-257.

24. D. Girlich and H.-D. Lüdemann. *Z. Naturforsch.* **1993**, *48c*, 407-413.

25. W. Schnauss, F. Fujara and H. Sillescu. *J. Chem. Phys.* **1992**, *97*, 1378-1389.

26. I. A. Farhat, J. R. Mitchell, J. M. V. Blanshard and W. Derbyshire. *Carbohydrate Polymers* **1996**, *30*, 219-227.

27. B. P. Hills. NMR studies of water mobility in foods. In *Water management in the design and distribution of quality foods*; Y. H. Roos, R. B. Leslie and P. J. Lillford, Eds.; Nottingham University Press: Nottingham, 1999; pp 107-134.

28. B. P. Hills and K. Pardoe. *Journal of Molecular Liquids* **1995**, *63*, 229-237.

29. S. Li, L. C. Dickinson and P. Chinachoti. *J. Agric. Food Chem.* **1998**, *46*, 62-71.

30. M. T. Kalichevsky, E. M. Jaroszkiewicz, S. Ablett, J. M. V. Blanshard and P. J. Lillford. *Carbohydrate Polymers* **1992**, *18*, 77-88.

31. D. Ehlich and H. Sillescu. *Macromolecules* **1990**, *23*, 1600-1610.

32. M. J. G. W. Roozen, M. A. Hemminga and P. Walstra. *Carbohydr. Res.* **1991**, *215*, 229-237.

33. M. J. G. W. Roozen and M. A. Hemminga. *J. Phys. Chem.* **1990**, *94*, 7326-7329.

34. M. T. Cicerone, F. R. Blackburn and M. D. Ediger. *J. Chem. Phys.* **1995**, *102*, 471-479.

35. F. R. Blackburn, C. Wang and M. D. Ediger. *J. Phys. Chem.* **1996**, *100*, 18249-18257.

36. D. Champion, H. Hervet, G. Blond, M. Le Meste and D. Simatos. *J. Phys. Chem. B* **1997**, *101*, 10674-9.

37. M. Le Meste and A. Voilley. *J. Phys. Chem.* **1988**, *92*, 1612-1616.

38. M. A. Hemminga and I. J. Van den Dries. Spin Label Applications to Food Science. In *Spin Labeling: The Next Millennium*; L. J. Berliner, Ed.; Pergamon Press:, 1997; pp in press.

39. M. A. Hemminga. *Chem. Phys. Lipids* **1983**, *32*, 323-383.

40. M. A. Hemminga, P. A. de Jager, D. Marsh and P. Fajer. *J. Magn. Reson.* **1984**, *59*, 160-163.

41. J. S. Hyde. *Methods Enzymol* **1978**, *49*, 480-511.

42. D. D. Thomas, L. R. Dalton and J. S. Hyde. *J. Chem. Phys.* **1976**, *65*, 3006-3024.

43. D. Marsh and L. I. Horváth. *J. Magn. Reson.* **1992**, *99*, 323-331.

2

Sensitivity of Saturation Transfer Electron Spin Resonance Extended To Extremely Slow Mobility in Glassy Materials[1]

Ivon van den Dries, Adrie de Jager, and Marcus Hemminga

ABSTRACT

A novel extension of the saturation transfer (ST) ESR technique that enables the determination of extremely long rotational correlation times of nitroxide spin labels up to values around 10^4 s is proposed. The method is based on the observation that the integral of ST-ESR spectra is sensitive to the spin-lattice relaxation time of the electron of the spin label, which in turn is directly dependent upon the rotational correlation time. The method is applied to the spin label TEMPOL (4-hydroxy-2,2,6,6-tetramethylpiperidine N-oxyl) in glycerol. From the known viscosity data and the related rotational correlation times of the TEMPOL spin label in glycerol, the rotational correlation times of unknown samples can be determined. The method is especially applicable to systems with a very high viscosity, such as glassy materials. The method is applied to a 20 wt % glucose-water mixture in the glassy state, giving a value for the highest limiting rotational correlation time of about 10^3 s at a temperature of 45 K below the glass transition temperature of this system. This is an extension by six decades for the rotational correlation time, as compared to the current application of ST-ESR.

INTRODUCTION

During the last years there has been an increasing interest in the study of molecular motions in glassy food materials [1]. Knowledge about the glass transition and physical properties of glassy materials is of crucial importance for the processing, quality, and storage stability of food. Furthermore, below the glass transition temperature, the very low molecular mobility of the matrix would predict a good food stability [2, 3]. Most of the basic work in this area has been carried out on sugar-water systems that are used as a model for food systems[1].

Electron spin resonance (ESR) spectroscopy and saturation transfer (ST) ESR have been shown to be suitable spectroscopic tools for obtaining information about the molecular mobility in sugar-water systems over a large range of temperatures, using small nitroxide spin-labeled molecules as probes [4-6]. Conventional ESR is sensitive in the motional region for values of the rotational correlation time τ_R between 10^{-11} and 10^{-8} s. In the motional region for $\tau_R > 10^{-7}$ s, ST-ESR is commonly used. ST-ESR is based on the diffusion and recovery of saturation between different portions of the spectrum [7, 8] in competition with field modulation. For the usual ST-ESR field modulation frequencies of around 50 kHz, the upper limit of sensitivity for rotational mobility is for $\tau_R \approx 10^{-3}$ s [7, 9], provided that there is sufficient recovery of saturation, which is determined by the spin-lattice relaxation time of the electron (T_1). At room temperatures, T_1 is about 1 µs for nitroxide spin labels [10], which is in the right range for ST-ESR spectroscopy. Beyond the upper limit, the ST-ESR spectra are no longer sensitive for the diffusion of saturation, because the dominating effect is the recovery of saturation, as given by T_1.

This article is based on the hypothesis that ST-ESR spectra are also sensitive to recovery of saturation with a limiting value of $T_1 \approx 10^{-3}$ s and that T_1 is only dependent on τ_R for $\tau_R > 10^{-3}$ s. By recent work of Robinson et al. [11] on the spin-lattice relaxation of nitroxide spin labels in glycerol-water solutions, it is

found that the spin-lattice relaxation time T_1 is proportional to $\tau_R^{1/8}$ for $\tau_R > 10^{-6}$ s, and it follows that T_1 is about 10^{-4} s at values for τ_R around 10^{-3} s. It may be expected that beyond the upper limit of sensitivity for rotational mobility ($\tau_R \approx 10^{-3}$ s) , ST-ESR spectra will still be sensitive to saturation recovery (T_1) in competition with field modulation until T_1 has a value of 10^{-3} s. Therefore the dependence of T_1 with τ_R provides an indirect means for measuring molecular mobility in this motional region.

In this paper, we have exploited this idea by studying ST-ESR spectra of the spin label 4-hydroxy-2,2,6,6-tetramethylpiperidine N-oxyl (TEMPOL) in glycerol in the temperature range from 140 to 280 K. From these experiments it is found that the ST-ESR spectra, as represented by the relative integrated intensity, indeed are (via T_1) sensitive to rotational correlation times $\tau_R > 10^{-3}$ s. From the known viscosity data and theoretically derived rotational correlation times of the TEMPOL spin label in glycerol, the relative integrated intensity of ST-ESR spectra of the TEMPOL spin label in glycerol can be used as a calibration for the rotational correlation times of unknown samples. The method is applied to a 20 wt% glucose-water mixture in the glassy state, giving a value for the highest limiting rotational correlation time of about 10^3 s at a temperature of 45 K below the glass transition temperature of this system. This method opens exciting new ways for obtaining information about rotational molecular motions in the glassy state. This is an extension by six decades for the rotational correlation time, as compared to the current application of ST-ESR.

MATERIALS AND METHODS

Preparation of solutions

Glycerol was mixed with the spin label 4-hydroxy-2,2,6,6-tetramethylpiperidine N-oxyl (TEMPOL, obtained from Sigma) and dried over phosphorpentoxide under vacuum for at least 2 weeks. Glucose was obtained from Jansen

13

Chimica. The glucose concentration was adjusted with water and an aqueous solution of the TEMPOL spin label. The final concentration of the TEMPOL spin label in the samples was 0.2 - 0.5 mg/ml. For the use in ESR and ST-ESR, the samples were sealed in 100 μl tubes (Brandt). The sample height was 5 mm. The capillaries were placed in 4 mm quartz ESR sample tubes. For the ESR experiments, the sample was carefully placed in the center of the microwave cavity. All samples were rapidly cooled to a temperature of about 140 K and subsequently measured during stepwise warming up.

Spectroscopy

ESR and ST-ESR spectra were recorded on a Bruker ESP 300E ESR spectrometer equipped with a TMH (Bruker) cavity and nitrogen temperature control. The temperature was measured with a small CuCo thermocouple close to the sample. The temperature accuracy is ±1.0 K. For conventional ESR the microwave power was set to 2 mW. The scan range, scan rate, time constant, and field modulation amplitude were adjusted so that distortion of the spectra was avoided. The rotational correlation time (τ_R) of weakly immobilised spin labels (10^{-11} s $< \tau_R < 10^{-9}$ s) was obtained from the relation [12]:

$$\tau_R = 6.5 \times 10^{-10} \, \Delta B_0 \left(\sqrt{h_C/h_H} - 1 \right) \qquad [1]$$

where h_H and h_C are the heights of the high field and central lines in the ESR spectra, respectively. ΔB_0 is the linewidth of the central line in Tesla (T). The rotational motion of the TEMPOL spin label is assumed to be isotropic.

For ST-ESR spectroscopy the second harmonic quadrature absorption signal was detected under the following conditions [10, 13]: field modulation amplitude 0.5 mT, microwave power 100 mW, and field modulation frequency 50 kHz. The phase was set with the self-null method [7].

The relation between the rotational correlation time τ_R and temperature of TEMPOL spin label in glycerol was determined in the following way:

14

1. Conventional ESR spectra of the TEMPOL spin label in anhydrous glycerol were recorded between room temperature and 373 K, and the rotational correlation time τ_R of the spin label was determined from the ESR spectra using Eq. [1]. It is generally assumed that the rotational behaviour of the spin label can be described with a modified Stokes-Einstein equation, given by [4, 14-16]

$$\tau_R = (\eta V/k_b T)\, k + \tau_0 \qquad\qquad [2]$$

where τ_R is the rotational correlation time, η is the solvent viscosity, k_b is Boltzmann's constant, V is the volume of the rotating molecule, T is the absolute temperature, and τ_0 is the zero viscosity rotational correlation time. The parameter k is a dimensionless interaction parameter, which is a measure of the coupling of the rotational motions of the spin label to the shear modes of the fluid. It has been found in many cases that the interaction parameter k << 1, and that k is independent of temperature and viscosity [4, 14, 17]. For the TEMPOL spin label, the volume $V = 0.180$ nm^3 [4], and for the spin label in glycerol it was found that $k = 0.09$ and that τ_0 is negligibly small. The data for the viscosity of glycerol were obtained from Ref. [18].

2. Since ST-ESR spectra were recorded in the temperature range from 140 to 280 K, the viscosities in this temperature range need to be known. However, viscosity data of anhydrous glycerol in the low-temperature region are published only for temperatures above 240 K [18]. Therefore, the known viscosity data at temperatures from 240 to 300 K were fitted to the empirical Williams-Landel-Ferry (WLF) equation [19]

$$log\frac{\eta}{\eta_g} = \frac{C_1\left(T - T_g\right)}{C_2 + \left(T - T_g\right)} \qquad\qquad [3]$$

to provide the viscosities at lower temperatures. In Eq. [3], T_g is the glass transition temperature of glycerol, and η_g the corresponding viscosity. It should be noted that Eq. [3] is only valid in the temperature range of about 100 K above T_g. The constants C_1 (-17.4) and C_2 (51.6 K) are universal constants of the WLF theory. Using Eq. [3], T_g was found to be 185 K, which is identical to the literature value [20, 21]. This validates the use of the universal values for the constants C_1 and C_2 in Eq. [3]. The resulting value for the viscosity η_g at the glass transition is 9.4×10^{11} Pas. By using Eqs. [2] and [3], the rotational correlation time τ_R of the TEMPOL spin label in glycerol can be calculated as a function of temperature.
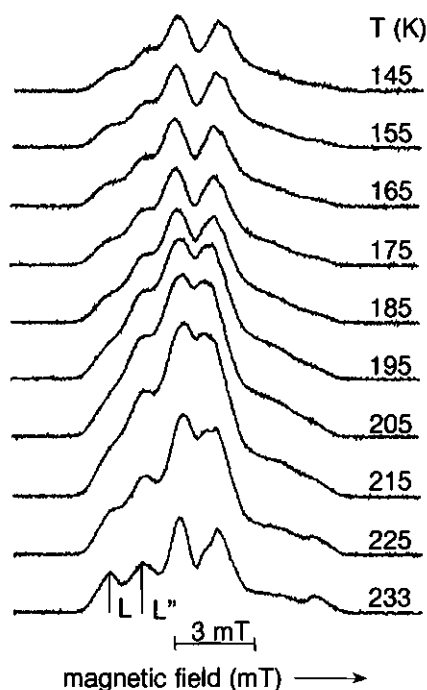
RESULTS

Figure 1 ST-ESR spectra of the TEMPOL spin label in pure glycerol at different temperatures (in K). The lineheights L and L" determine the characteristic low-field ratio L"/L.
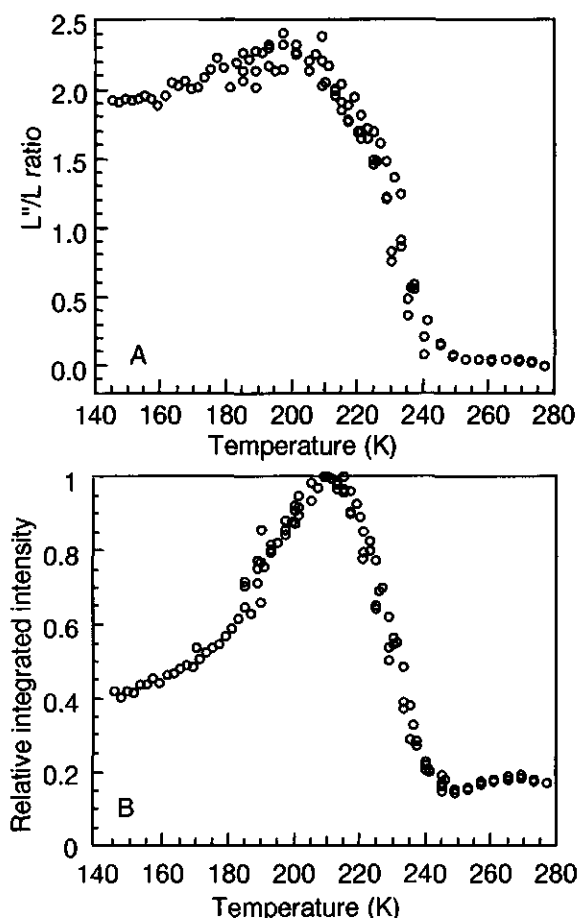
Figure 2 The L"/L ratio (a) and the relative integrated intensity Irel (b) of ST-ESR spectra of the TEMPOL spin label in glycerol as a function of temperature. The results of four separate experiments are shown.

ST-ESR spectra of the TEMPOL spin label in glycerol (Fig. 1) are measured as a function of temperature from 140 to 280 K. The low-field ratio (L"/L) of these spectra increases with decreasing temperature and reaches a maximum value of 2.2 at a temperature of about 200 K (Fig. 2a). The low-field ratio decreases again with a further decrease in temperature. A closer look at the spectra reveals quite a different lineshape at temperatures above and below 200 K (Fig. 1). On decreasing the temperature from room temperature, the lineshape changes toward an absorption-type ESR spectrum at a temperature
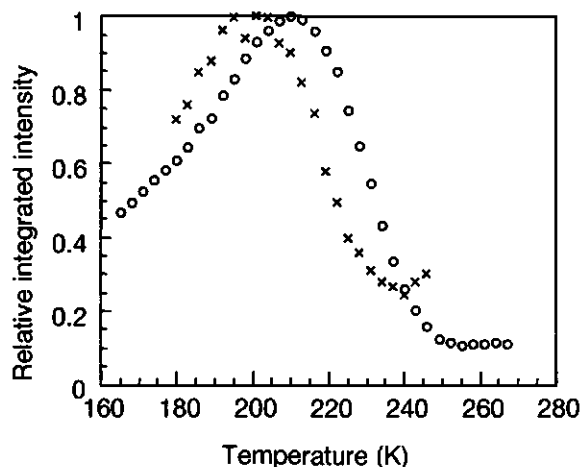
17

Figure 3 The relative integrated intensity Irel of ST-ESR spectra as a function of temperature with modulation frequencies of 100 kHz (x) and 12kHz (o)

of about 200 K in which the lineheights L" and L can not be well distinguished. On further decreasing the temperature, the lineheights L" and L become more distinguished again. In Fig. 2b, the relative integrated intensity I_{rel} of the ST-ESR spectra is shown as a function of temperature. To calculate the integrated intensity, the ST-ESR spectra in Fig. 1 were integrated by the computer. The relative integrated intensity is expressed as a fraction of the maximal integral. The curve in Fig. 2b shows a clear maximum at a temperature of 210 K. The temperature of this maximum shifts to a lower temperature if an modulation frequency of 12 kHz is used in stead of a modulation frequency of 50 kHz. Using a 100kHz modulation frequency, the maximum occurs at a slightly higher temperature (Fig. 3). The lineheight ratio L"/L and relative integrated intensity I_{rel} are replotted as a function of the rotational correlation time τ_R in Fig. 4, by substituting the temperature for the rotational correlation time as described by Eqs. [2] and [3]. Because the viscosity of glycerol can be calculated only for temperatures above T_g (see Eq. [3]), the range of τ_R is from 10^{-6} to 5×10^4 s.

Note that in Fig. 4a the lineheight ratio L"/L levels off and loses motional sensitivity for values of τ_R above 10^{-2} s, whereas the relative integrated intensity
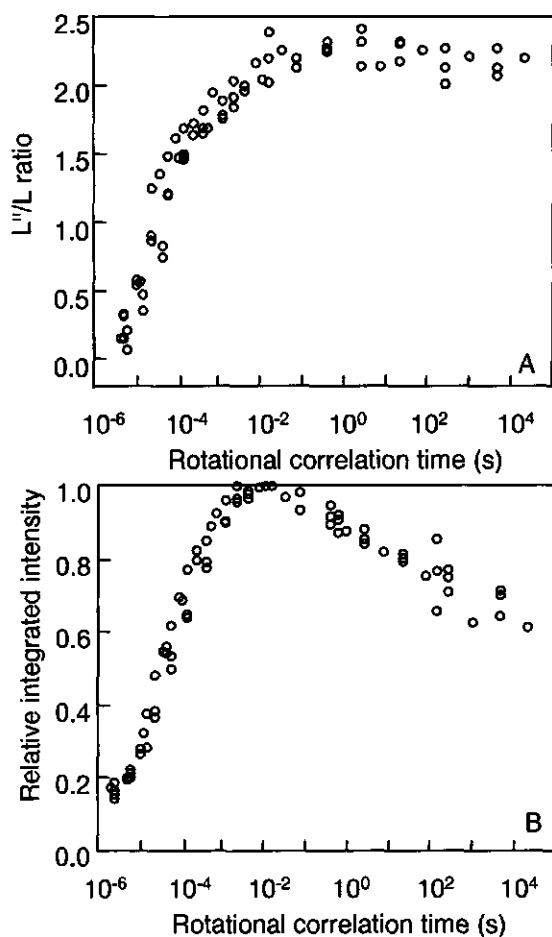
Figure 4 The L"/L ratio (a) and the relative integrated intensity Irel (b) of the ST-ESR spectra of the TEMPOL spin label in glycerol as a function of the rotational correlation

I_{rel} (Fig. 4b) still shows a peak around this τ_R value. However, for values of τ_R below 10^{-2} s, the slope is much steeper than for values above this value, indicating that the sensitivity of the relative integrated intensity I_{rel} for motion is decreased for very slow motions.

By using the ST-ESR data obtained from the TEMPOL spin label in glycerol as a calibration, the rotational correlation time of the TEMPOL spin label in a 20 wt % glucose-water mixture is determined as a function of temperature (Fig. 5). For comparison, the results arising from both the relative integrated intensity I_{rel}
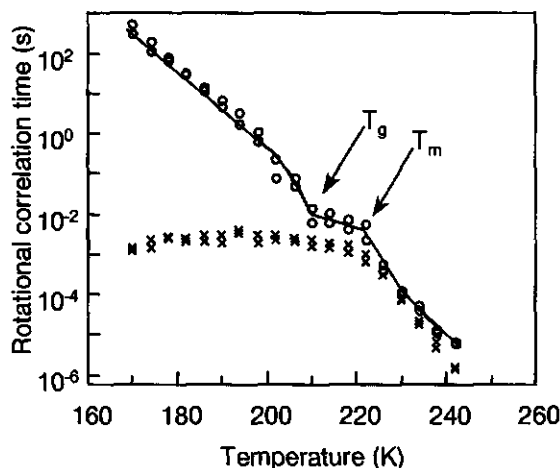
Figure 5 Rotational correlation time τ_R of the TEMPOL spin label in a 20 wt% glucose-water system analyzed using the L"/L ratio (x) and the relative integrated intensity Irel (o) obtained in glycerol (Fig. 3). The glass transition temperature Tg (210 K) and the melting temperature T_m (223 K) are indicated with arrows.

and the L"/L ratio of the ST-ESR spectra are plotted, showing that the relative integrated intensity I_{rel} is much more sensitive for long rotational correlation times than the L"/L ratio.

DISCUSSION

The goal of this study is to develop ESR methods that can be used to determine molecular motion in high-viscosity systems, such as glassy sugar-water systems and foods. Conventional ESR and ST-ESR spectroscopy using nitroxide spin labels have already been shown to be suitable methods for this purpose: the spin labels provide information about their local environment, and ESR spectroscopy is especially powerful in obtaining data about molecular mobilities that cannot easily be obtained in alternative ways [4-6, 22, 23]. ST-ESR is based on rotational diffusion or recovery of saturation in competition with the field modulation. For ST-ESR, employing field modulation frequencies around 50 kHz, the upper limit of sensitivity for rotational mobility is usually found for rotational correlation times $\tau_R \approx 10^{-3}$ s [7, 9, 10]. This article is based on the hypothesis that ST-ESR spectra are also sensitive to recovery of saturation with

20

a limiting value of $T_1 \approx 10^{-3}$ s and that T_1 is only dependent on τ_R for $\tau_R > 10^{-3}$ s. Recently it has been observed that the spin-lattice relaxation time of the electron (T_1) of the TEMPOL spin label in glycerol-water mixtures increases with τ_R and has a value of 10^{-4} s at the limiting value of $\tau_R \approx 10^{-3}$ s [11]. Thus it may be expected that in the motional region for $\tau_R > 10^{-3}$ s, ST-ESR spectra will still be sensitive to saturation recovery (T_1) in competition with field modulation. This would provide a new indirect way of quantifying rotational correlation time τ_R in this motional region.

In order to analyze ST-ESR spectra, a spectral characteristic, sensitive for rotational diffusion, is related to calculated values of τ_R in a reference sample. In our study we have used the TEMPOL spin label in glycerol as a calibration system for carbohydrate-water systems. Glycerol has a close chemical resemblance to sugars, and it can be used as a model compound for glassy sugar-water systems. Furthermore, the viscosity of glycerol is known over a large temperature range. We used a very broad temperature range to study the ST-ESR spectra of the TEMPOL spin label in glycerol (Fig. 1), to cover a large range of molecular motions and spin-lattice relaxation times. At low temperatures the characteristic transfer features of ST-ESR spectra disappear because large rotational correlation times inhibit transfer of magnetization at time scale of the modulation frequency. At these low temperatures overmodulated spectra of T_1 recovery are measured.

The analysis of the ST-ESR spectra was carried out in two different ways e.g. by using the low-field spectral ratio L"/L [7] or the integrated intensity [24-26]. Both spectral characteristics have been shown to yield equivalent results in determining rotational correlation times τ_R up to $\tau_R \approx 10^{-4}$ s [24, 27]. Our results are plotted in Fig. 2. On decreasing the temperature both the low-field spectral ratio L"/L (Fig. 2a) and the relative integrated intensity I_{rel} (Fig. 2b) reach a maximum, but after passing the maximum, the temperature dependence of the L"/L ratio is relatively small as compared to the relative integrated intensity I_{rel}. It

should be noted that around a temperature of 200 K, the L''/L ratio is difficult to determine from the ST-ESR spectra (Fig. 1), which is represented by the scattered values in this temperature range (Fig. 2a). Below a temperature of 200 K, the relative integrated intensity I_{rel} (Fig. 2b) has a more pronounced change with temperature and lacks the scattering problem. For this reason the integrated intensity has the best properties to be used as a spectral characteristic below a temperature of 200 K. Apart from a better reproducibility and a stronger temperature dependence, another advantage of the integrated intensity is that possible line broadening effects are not reflected in the relative intensity I_{rel}. Therefore, the relative integrated intensity I_{rel} is exclusively affected by τ_R and T_1. It should be noted that a disadvantage of the use of the relative integrated intensity I_{rel}, which is normalised to the maximum, is that the whole temperature range must be studied.

Maximal effects of rotational motion and spectral recovery in ST-ESR spectra arise, if the rotational correlation time τ_R, spin-lattice relaxation time T_1, and angular field modulation frequency ω_m obey the following equation [7, 8, 10]

$$\tau_{R, opt} \approx 1/(\omega_m), \text{ and } T_{1, opt} \approx 1/(\omega_m) \tag{4}$$

where $\tau_{R, opt}$ and $T_{1, opt}$ are the optimal values for τ_R and T_1, respectively. The maximal sensitivity for motion at a field modulation frequency of 50 kHz, as used in our ST-ESR experiments, is then expected for a value of τ_R, opt of about 10^{-5} s. The sensitivity range is usually taken as a range plus or minus two decades, giving $\tau_R \approx 10^{-3}$ s as a higher limit. In Fig. 2b, a maximum is seen in I_{rel} at a temperature of 210 K. From Eqs. [2] and [3], it can be calculated that at around this temperature the rotational correlation time τ_R has a value of about 10^{-2} s. By extrapolating the T_1 data of the TEMPOL spin label in glycerol-water systems versus τ_R [11], it is then estimated that T_1 is about 10^{-4} s, although 100% glycerol is used in stead of glycerol water mixtures. At a field modulation frequency of 50 kHz, this is in the sensitivity range for T_1, and relaxation

processes will still affect the ST-ESR lineshape.

Following well-known theories of AC electric circuits and viscoelastic response, it can be anticipated that the out-of-phase response given by the relative integrated intensity I_{rel} of the ST-ESR spectra upon the angular field modulation frequency $\omega_m = 2\pi\nu_m$ and with a characteristic time T_1 can be described by

$$I_{rel} \propto \frac{\omega_m T_1}{1 + (\omega_m T_1)^2} \qquad [5]$$

In Eq. [5] it can be seen that effects of the relaxation time T_1 on I_{rel} will be most efficiently detected, if $\omega_m T_1 \sim 1$. This is reflected by the top of the curve in Fig. 2b. Using a smaller modulation frequency, the temperature of the maximum relative intensity decreases (Fig. 3) because T_1^{-1} decreases with decreasing temperature[11].

Since it may be expected that T_1 continues to increase with decreasing temperatures (T_1 varies with $\tau_R^{1/8}$ for $\tau_R > 10^{-3}$ s) [11], the ST-ESR lineshape will change as a function of temperature until a final limit for sensitivity to T_1 is reached at a temperature somewhere below a temperature of 140 K. This T_1 effect is illustrated by the decrease of the relative integrated intensity I_{rel} for temperatures below 210 K (Fig. 2b) and follows from Eq. 5. The effect can also be observed in the temperature dependence of L"/L (Fig. 2a), but it is less pronounced.

The lineheight ratio L"/L and relative integrated intensity I_{rel} can be directly related to the rotational correlation time τ_R, as is presented in Fig. 4. Because the viscosity of glycerol, as described by Eq. [3] can be calculated only for temperatures above the glass transition T_g of glycerol (185 K), the range of values for τ_R is ranging from 10^{-6} to 5×10^4 s. From a comparison of Fig. 4a and b, it can be seen that the relative integrated intensity is much more sensitive for values of τ_R from 10^{-2} to 10^4 s, as compared to the L"/L ratio. Therefore, the relative integrated intensity I_{rel} as given in Fig. 4b is the best parameter to be

23

used as a calibration for rotational correlation times τ_R of the TEMPOL spin label in unknown samples, as compared to the L"/L ratio. It should be noted, however, that because of the small slope of I_{rel} in Fig. 4b for values of τ_R above about 10^{-2} s, the errors in τ_R will be relatively large.

In Fig. 4 its is assumed that the rotational correlation time τ_R can be calculated from Eqs. [2] and [3]. This implies (1) that the viscosity follows the Williams-Landel-Ferry (WLF) theory and (2) that the modified Stokes-Einstein Eq. [2] is valid in supercooled liquids. It has been observed in glycerol that in general dynamical processes follow the WLF Eq. [3] [21, 28, 29]. This is also true for the rotational correlation times obtained from NMR hole-burning experiments in glycerol [20]. This means that the temperature dependence of the viscosity is well described by Eq. [3], and that the interaction parameter k in Eq. [2] is temperature independent.

It is interesting to compare our rotational correlation time data obtained with the TEMPOL spin label in glycerol with those of glycerol itself [20]. For glycerol at the glass transition temperature T_g (185 K), it has been found that τ_R is 1.0×10^3 s [20]. In our case, we calculate for the TEMPOL spin label a value for τ_R of 4.0×10^3 s, which is in the same order of magnitude. Using the molecular volumes of glycerol as given by Bondi [30], the interaction parameter k of glycerol can be calculated to be 0.03. For the TEMPOL spin label the interaction parameter k is a factor of 3 larger (0.09). This difference can be explained by the fact that a TEMPOL spin label is slightly larger than a glycerol molecule (the average radii are 0.35 and 0.27 nm, respectively). It has been observed that for small molecules with an average radius between 0.2 and 0.6 nm, the experimental rotational diffusion coefficient is systematically higher than calculated from the modified Stokes-Einstein; this discrepancy increases as the molecule becomes smaller [17].

To illustrate the possibilities of this ST-ESR method, the rotational correlation times τ_R of the TEMPOL spin label in glycerol determined from the L"/L ratio

and the relative integrated intensity I_{rel} were used as a calibration to determine unknown τ_R values in a 20 wt% glucose-water sample (Fig. 5). Upon cooling this sample a phase separation takes place, because ice is formed. Upon rewarming such a sample, the melting of ice starts at the melting temperature T_m. The process of ice formation upon cooling concentrates the remaining glucose solution containing the spin label, and finally the supersaturated solution undergoes a glass transition at a temperature T_g of 216 K [1]. The low mobility below this glass transition temperature is expected to allow a prolonged storage stability of the glass, and therefore is an important object of study in food science.

From Fig. 5, it is seen that the glass transition temperature T_g (210 K) and the melting temperature T_m (223 K) are well identified as breaks in the plot determined from the relative integrated intensity I_{rel}. These values of T_g and T_m are in agreement with the literature [1]. Furthermore, τ_R values can be determined at temperatures far below the glass transition temperature T_g, and τ_R can be determined in the glassy state up to a value of about 10^3 s. In contrast, the L"/L ratio levels off at a value of about 2.1, giving τ_R values around 10^{-3} s. At these values the limit of sensitivity for mobility for the L"/L ratio is reached. This effect can be explained by realizing that the L"/L ratio is almost insensitive to T_1 effects, and that changes in T_1 are the main cause for sensitivity for motion for $\tau_R > 10^{-3}$ s. This means that by using the relative integrated intensity I_{rel} of ST-ESR spectra, the range of sensitivity for mobility is extended with six orders of magnitude, as compared to using the L"/L ratio.

In conclusion, we have shown that small stable nitroxide spin labels incorporated in a glassy host material reflect the motional properties of the host. Until now, the motional sensitivity of ST-ESR was limited to slow molecular motions around a rotational correlation time of about 10^{-3} s. This value does not always reflect the glassy state of the host, and therefore limits the motional information that can be obtained about the glassy state. Here, we introduce a

new approach of ST-ESR, which enables us to measure rotational correlation times of spin labels up to values of 10^3 s. This is a major breakthrough in the ST-ESR technique, giving us an increase by six decades as compared to previous methods. Taking into account that the lower limit of conventional ESR is for values of rotational correlation times τ_R of about 10^{-11} s, our experiments show that *a single set of equipment for ESR spectroscopy is able to cover an immense range of rotational molecular motions.*

This observation makes ESR spectroscopy an extremely versatile technique that enables one to provide motional knowledge about the glassy state. Since our work is aimed at the study of the stability and preservation of food and pharmaceuticals, such motional information might help technologists to develop better ways for storage and manufacturing. In addition, it could give some clues about the long-term stability of biological materials (i.e. seeds).

ACKNOWLEDGMENTS

REFERENCES

1. Y. Roos *Phase Transitions in Foods*; Academic Press: San Diego, 1995.

2. F. Franks *Biophysics and Biochemistry at Low Temperatures*; Univ. Press: Cambridge, 1985; Vol. Chapter 3.

3. H. Levine and L. Slade. Glass transitions in foods. In *Physical Chemistry of Foods*; H. G. Schwartzenberg and R. W. Hartel, Eds.; Dekker: New York, 1992; pp 83-221.

4. M. J. G. W. Roozen and M. A. Hemminga. *J. Phys. Chem.* **1990**, *94*, 7326-7329.

5. M. J. G. W. Roozen, M. A. Hemminga and P. Walstra. *Carbohydr. Res.* **1991**, *215*, 229-237.

6. M. A. Hemminga, M. J. G. W. Roozen and P. Walstra. Molecular motions and the glassy state. In *The Glassy State in Foods*; J. M. V. Blanshard and P. J. Lillford, Eds.; Nottingham University Press: Nottingham, 1993; pp 157-171 (Chapter 7).

7. D. D. Thomas, L. R. Dalton and J. S. Hyde. *J. Chem. Phys.* **1976**, *65*, 3006-3024.

8. M. A. Hemminga. *Chem. Phys. Lipids* **1983**, *32*, 323-383.

9. B. H. Robinson, H. Thomann, A. H. Beth, P. Fajer and L. R. Dalton *The phenomenon of magnetic resonance: theoretical considerations*; CRC; Boca Raton, Fl: , 1985.

10. M. A. Hemminga and P. A. De Jager. Saturation transfer spectroscopy of spin labels: techniques and interpretation of spectra. In *Biological Magnetic Resonance. Spin Labeling - Theory and Applications*; L. J. Berliner and J. Reuben, Eds.; Plenum Press: New York, 1989; Vol. 8; pp 131-178.

11. B. H. Robinson, D. A. Haas and C. Mailer. *Science* **1994**, *263*, 490-493.

12. P. F. Knowles, D. Marsh and H. W. E. Rattle *Magnetic Resonance of Biomolecules*; Wiley: London, 1976.

13. M. A. Hemminga, P. A. de Jager, D. Marsh and P. Fajer. *J. Magn. Reson.* **1984**, *59*, 160-163.

14. R. E. D. McClung and D. J. Kivelson. *Chem. Phys.* **1968**, *59*, 3380-3391.

15. D. Kivelson, M. G. Kivelson and I. Oppenheim. *J. Chem. Phys.* **1970**, *52*, 1810-1821.

16. J. L. Dote, D. Kivelson and R. N. Schwartz. *J. Phys. Chem.* **1981**, *85*, 2169-2180.

17. J. T. Edward. *J. Chem. Educ.* **1970**, *47*, 261-270.

18. TEMP *Physical properties of glycerine and its solutions*; Glycerine Producers' Association: New York, 1969.

19. M. L. Williams, R. F. Landel and J. D. Ferry. *J. Am. Chem. Soc.* **1955**, *77*, 3701-3707.

20. P. L. Kuhns and M. S. Conradi. *J. Chem. Phys.* **1982**, *77*, 1771-1982.

21. R. M. Diehl, F. Fujara and H. Sillescu. *Europhys. Lett.* **1990**, *13*, 257-62.

22. M. J. G. W. Roozen and M. A. Hemminga. *Spec. Publ. - R. Soc. Chem.* **1991**, *82*, 531-536.

23. M. A. Hemminga and I. J. Van den Dries. Spin Label Applications to Food Science. In *Spin Labeling: The Next Millennium*; L. J. Berliner, Ed.; Pergamon Press:, 1997; pp in press.

24. L. I. Horváth and D. Marsh. *J. Magn. Reson.* **1983**, *54*, 363-373.

25. L. I. Horváth, P. J. Brophy and D. Marsh. *Biochim. Biophys. Acta* **1993**, *1147*, 277-280.

26. C. A. Evans. *J. Magn. Reson.* **1981**, *44*, 109-116.

27. D. Marsh and L. I. Horváth. *J. Magn. Reson.* **1992**, *99*, 323-331.

28. W. Schnauss, F. Fujara and H. Sillescu. *J. Chem. Phys.* **1992**, *97*, 1378-1389.

29. F. Fujara, W. Petry, R. M. Diehl, W. Schnauss and H. Sillescu. *Europhys. Lett.* **1991**, *14*, 563-568.

30. A. Bondi. *J. Phys. Chem.* **1964**, *68*, 441-451.

3

Mobility in maltose-water glasses studied with ^{1}H-NMR[1]

Ivon van den Dries, Dagmar van Dusschoten, and Marcus Hemminga

ABSTRACT

We have studied the molecular mobility of the water and carbohydrate protons in maltose samples as a function of water content and temperature using ^{1}H NMR. In the NMR signal, slow decaying and fast decaying fractions of protons are distinguished as arising from mobile and immobile ($\tau_c > 3$ µs) protons, respectively. The assignment of these fractions in terms of water and maltose protons is temperature dependent. By analyzing the relaxation behavior of the mobile protons, the mobility of the water molecules is determined. The mobility of water molecules increases with water content and temperature, and at the glass transition, a small break in mobility is observed, indicating that the water molecules slightly sense the glass transition. The method of second moments gives information about the mobility of the immobile protons. Upon cooling, the glass transition is marked by a decrease in the temperature dependence of the mobility of the hydroxyl protons of maltose. This suggests that a stable hydrogen-bond network between the sugar molecules is formed at the glass transition temperature that immobilizes the hydroxyl groups. Water disrupts this network, and this results in a higher mobility of the hydroxyl protons of maltose. The more water the stronger is this plasticizing effect.

INTRODUCTION

During the last few years there has been an increasing interest in the study of molecular motions in glassy food materials [1]. Discontinuities in macroscopic properties such as the viscosity, specific heat, and specific volume characterize the glass transition. At a molecular level, an interpretation of these macroscopic discontinuities is still lacking, but the macroscopic changes must be related to a change of molecular mobility. Several techniques can be used to study molecular mobility around the glass transition temperature such as electron spin resonance (ESR) [2-4], fluorescence [5, 6], dielectric relaxation, [7] and nuclear magnetic resonance (NMR) techniques [8-11]. From these studies, it is clear that although the mobility of the glass-forming molecules decreases strongly around the glass transition temperature, small molecules such as fluorescent or spin probes remain relatively mobile [2-5, 8, 9, 12-16].

In the present work, we focus on the molecular mobility in maltose-water systems. It is known that water reorients relatively independent of the carbohydrate matrix,[9] resembling other small molecules in a matrix. Although water molecules only slightly sense the glass transition of the matrix, their presence largely depresses the glass transition temperature. The molecular mechanism of this plasticizing effect is studied with proton NMR. With NMR immobile (τ_c >10 µs) and mobile protons are distinguished, and can be roughly assigned to hydroxyl and ring protons of maltose and water protons. By analysis of the relaxation behavior of the mobile protons, the mobility of the water is studied. The method of second moments is used to obtain information about the mobility of the immobile protons around the glass transition temperature. On the basis of the results of mobility of protons around the glass transition temperature, a molecular mechanism of plasticization is proposed.

MATERIALS AND METHODS

Preparation of maltose-water samples

Maltose-monohydrate (Merck) was mixed with the appropriate amount of water in a 5 mm NMR tube to adjust the content of maltose to 80, 90, and 93 wt %. For the 95 wt % sample, maltose monohydrate was used without addition of water. The NMR tubes were sealed to prevent water evaporation. The maltose-water samples were melted in an oil bath at a temperature of about 420 K. The melting time was as short as possible to obtain a homogeneous melted sample without browning by degradation of the maltose. Melted maltose samples were quickly cooled and stored below their respective glass transition temperature. Maltose with deuterated hydroxyl groups was prepared by dissolving the monohydrate (1 g) in D_2O (5 ml) and subsequent freeze-drying before adjusting the water content with D_2O. The glass transition temperature of the deuterated samples was measured with differential scanning calorimetry (DSC) and compared with literature values [7]. The D_2O contents were 7 wt % and 21 wt %.

NMR Spectroscopy

^{1}H NMR measurements were performed on a Bruker AMX 300 spectrometer equipped with a Bruker 5 mm proton probe operating at a resonance frequency of 300.13 MHz. The temperature was regulated with a nitrogen temperature control. In this way, the temperature stability was within ±0.5 K. A spectral width of 500 kHz was used. The duration of the 90° pulse was 6-7 μs. The presented free induction decays (FID) are averages of 8 scans having 2048 data points. Cross relaxation rates were measured with the Goldman Shen pulse sequence [17, 18]. This pulse sequence of three $90_x°$ pulses makes use of the difference in spin-spin relaxation between fast and slow relaxing protons.

For the analysis of the NMR data at low temperatures, the FIDs F(t) were fitted to the following equation:

$$F(t) = A \exp\left(\frac{-a^2 t^2}{2}\right)\frac{\sin bt}{bt} + B \exp\left(\frac{-t}{T_{2m}}\right)$$ (1)

In this equation, the parameters A and B represent the contributions of the immobile and mobile protons in the sample, also presented by the integral of the broad and sharp line shape parts of the NMR spectrum, respectively (see Fig. 1A and B). Parameter T_{2m} is the spin-spin relaxation time of the mobile proton fraction. The NMR spectrum of the immobile proton fraction is assumed to be a rectangular line shape with a total width 2b, convoluted with a gaussian line shape with a standard deviation given by parameter a [19, 20].

For a resonance curve described by a normalized shape function $f(\omega)$ with a maximum at a frequency ω_0, the second moment M_2 with respect to the point ω_0 is defined as [19]:

$$M2 = \int (\omega - \omega_0)^2 f(\omega)\partial\omega$$ (2)

In our systems, the second moment is not used for the whole system but only for the broad part of the line shape that arises from the immobile proton fraction. The second moment M2 of the broad line shape, which is a measure of the strength of the dipolar interactions, is calculated from the fit parameters a and b by the following equation19:

$$M_2 = a^2 + \frac{1}{3}b^2$$ (3)

On increasing the temperature, the dipolar interactions start to average and the broad component of the NMR spectrum sharpens up. As long as the FIDs show oscillations, characteristic for the rectangular line shape of the immobile proton

fraction, they are well fitted by Eq. 1. Finally, the oscillatory character of the FID is lost, and the FIDs are fitted to a biexponential function.

RESULTS

The FIDs of a 80 wt % maltose-water sample at various temperatures are shown in Fig. 1A, and the corresponding NMR spectra are shown in Fig. 1B. The NMR spectra at low temperature consist of a sharp line shape, arising from
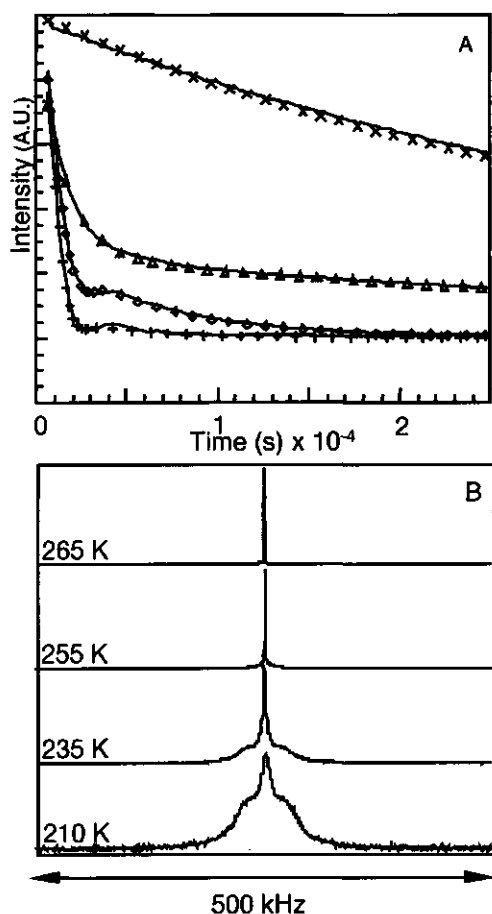

Figure 1 Free Induction Decays (FIDs) of 80 wt % maltose-water samples (A) and the corresponding Fourier transformed NMR spectra (B). For temperatures below 250 K the experimental FIDs are fitted to Eq. 1, whereas at higher temperatures a biexponential function is used.
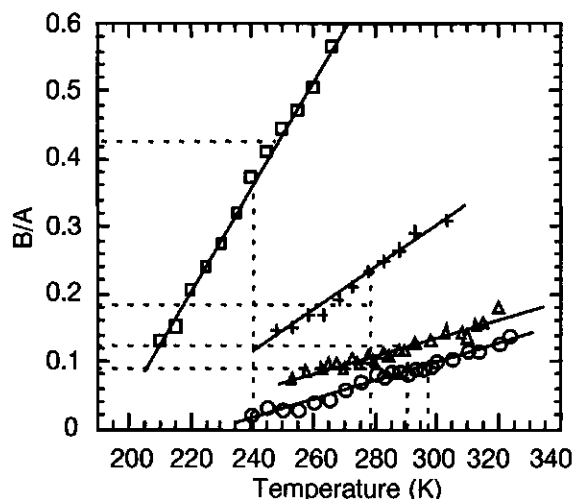
33

Figure 2 The ratio of the mobile (B) and immobile (A) proton fractions as a function of temperature for 95 (circles), 93 (triangles), 90 (crosses), and 80 wt % (squares) maltose samples. The straight lines are linear fits through the data points. The glass transition temperatures are indicated with dashed vertical lines. The dashed horizontal lines indicate the calculated values of B/A from Table 1.

relatively mobile protons, superimposed on a broad line shape, arising from immobile protons. The ratio of the mobile (B) and immobile (A) proton fractions in various maltose-water samples, as determined from fitting the FID to Eq. 1, is shown versus temperature in Fig. 2. For all samples, the ratio B/A increases almost linearly with increasing temperature, indicating that protons gradually go over from the immobile to the mobile fraction. No breaks are observed at the glass transition temperatures T_g[7], which are indicated by the vertical lines in Fig. 2. With increasing water content the slope of the lines increases.

For the 80 wt % maltose-water sample at a temperature of 255 K (Fig. 1), the typical characteristic of the broad line shape has completely disappeared and both line shape contributions have strongly sharpened up. In this case, Eq. 1 can no longer be used for the analysis of the FID and a biexponential fit is used instead. All data shown are fitted to Eq. 1, except for the samples with 80 wt % maltose at temperatures higher than 250 K and for the samples with 90 wt % maltose at temperatures above 300 K.
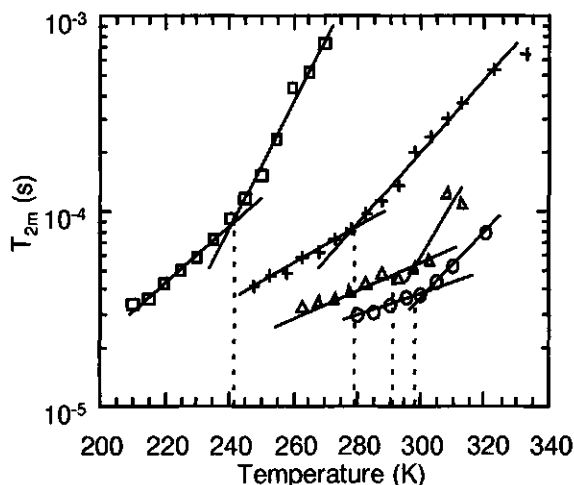
Figure 3 The relaxation time of the mobile protons (T2m) versus for 95 (circles), 93 (triangles), 90 (crosses), and 80 wt % (squares) maltose samples. The straight lines are linear fits through the data points. The glass transition temperatures are indicated with dashed vertical lines.

The glass transition temperatures are indicated with dashed vertical lines. The spin-spin relaxation time of the mobile protons, T_{2m}, obtained from the analysis of the FIDs is plotted in Fig. 3. In all cases, an increase of T_{2m} is observed at higher temperatures and water contents, resulting in a sharpening of the line shape of the mobile protons. Also, in this figure a rapid increase occurs in T_{2m} around T_g, indicated by the vertical lines. It is remarkable that T_{2m} at T_g increases with increasing water content, resulting in a sharper line shape, although the temperature decreases.

From the parameters a and b deduced from the fits of the FIDs with Eq. 1, the second moment M_2 of the broad line shape is calculated using Eq. 3. For samples with a low water content, the values of the second moment were also calculated using the integral method (Eq. 2) to check the validity of Eq. 3. The values of M_2 were comparable, and therefore, all data on M_2 of the immobile fraction are obtained with Eq. 3. The results are shown in Fig. 4 as a function of water content and temperature for protonated as well as for deuterated
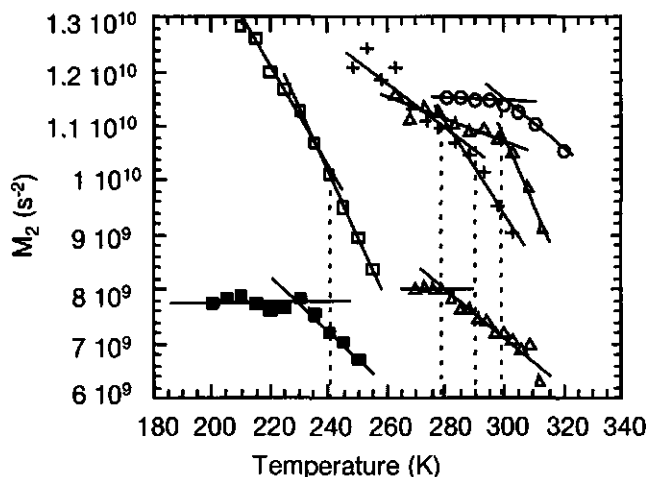
35

Figure 4 The second moment of the immobile protons (M_2) versus temperature for 95 (circles), 93 (triangles), 90 (crosses), and 80 wt % (squares) maltose samples. The second moment of solid protons in deuterated samples (93 and 79 wt %) is shown with corresponding filled symbols. The straight lines are linear fits through the data points. The glass transition temperatures are indicated with dashed vertical lines.

maltose-water systems. Higher values of M_2 are observed for the protonated samples (open symbols) as compared to the deuterated samples (filled symbols). Around the glass transition temperature T_g, indicated with vertical lines, breaks in M_2 are observed. Below T_g, a plateau value of M_2 is reached in both deuterated samples and the protonated 95 wt % maltose-water sample. In the other protonated samples, the increase of M_2 with decreasing temperature below T_g is larger if the sample contains more water. Below T_g, higher values of M_2 are reached on increasing water contents.

The cross relaxation rates in maltose-water systems, as determined with the Goldman Shen pulse sequence, [17, 18] are on the order of 10^3 s^{-1}. The cross relaxation rates slightly decrease with temperature and water content.

36

DISCUSSION

In this paper it is our aim to investigate the physical state and dynamics of the water and maltose molecules in concentrated maltose-water samples using ^{1}H NMR. The water content ranges between 5 and 20 wt % water. This corresponds to an average number of water molecules per maltose molecule in the range of 1 to 4.75, respectively. Under these conditions, all water molecules are unfreezable. The chemical structure of maltose is shown in Fig. 5. The protons of maltose can be divided in three groups: ten protons directly bound to the glucose rings, four CH_2 protons of the exocyclic groups, and eight hydroxyl protons. The mobility of the ring protons is thought to follow the overall mobility of the maltose molecule as a whole. The CH_2 and hydroxyl protons may have a higher albeit restricted mobility because they are remote from the ring and therefore have an additional degree of motional freedom. Furthermore, the hydroxyl protons have the ability to exchange with the water protons and to form hydrogen bonds with the water molecules and with other OH groups.

To discuss the dynamics of the water and sugar protons, it is desirable to know which part of the ^{1}H NMR signal decay can be ascribed to the water and which part to maltose protons. In the free induction decay (FID), slow decaying and fast decaying fractions of protons are arising from mobile and immobile protons, respectively. In the following, the assignment of the slow and fast
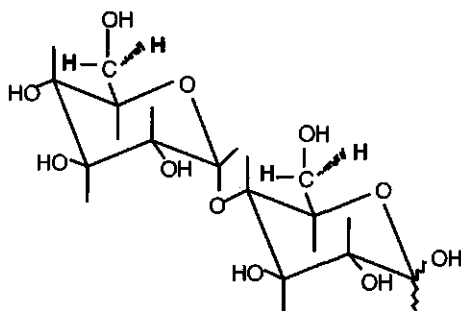

Figure 5 Molecular structure of maltose. The 8 hydroxyl protons (plain) and the 4 exocyclic protons (bold) are shown.

decaying part of the FID to water and sugar protons will be considered first, followed by a discussion of the transverse relaxation behavior (T_{2m}) of the mobile protons. Finally the second moment (M_2) of the immobile protons is discussed.

In Fig. 1B typical examples of low temperature ^{1}H NMR spectra are shown for an 80 wt % maltose-water sample. The broad spectral component arises from immobile protons and the relatively sharp peak, which is superimposed on it, arises from the mobile protons. The broad spectral component is the result of a distribution of static unaveraged proton dipole-dipole interactions in the sample. This results in a oscillatory behavior of the FID, where the frequency of the oscillations is a measure of the strength of the dipole interactions. The first part of the FID is then described by the damped sinusoidal part of Eq. 1. A similar FID was fitted using an equation in which the gaussian part of Eq. 1 was replaced by an exponential. [11] Comparing both fits we found that residual plots of the FID are best when using Eq. 1. The sharp line shape is well described by a lorentzian line shape, characterized by a width at half height given by $\Delta = (\pi T_{2m})^{-1}$. The lower limiting value of T_{2m} to describe the line shape with this equation is 2×10^{-5} s, which is about the width of the broad spectral component (Fig. 1). This corresponds to an upper limit of the correlation time τ_c of 3×10^{-6} s calculated using the Bloembergen-Purcell-Pound theory[19]. Protons with τ_c values above 3×10^{-6} s will be part of the broad line shape and will be called immobile or solid in the following discussion.

^{1}H NMR signals of carbohydrate-water mixtures studied previously were divided into a slowly relaxing part and a fast relaxing part. The slowly relaxing fraction was often identified as originating from the water protons and the fast relaxing fraction from the carbohydrate protons, although it was noted that hydroxyl protons of the sugar could contribute to the slowly relaxing decay by

38

chemical exchange. [9, 11, 21-23] Recently, it was observed in 93 wt % starch-water mixtures that some water molecules were relaxing fast at sub-zero temperatures[24]. This indicates that the immobile and mobile protons cannot be simply assigned to carbohydrate and water protons, respectively. This is also illustrated in Fig. 2, which shows that the ratio of amplitudes of the mobile (B) and immobile (A) fractions (Eq. 1) is temperature dependent.

The ratio of water protons and maltose protons can be calculated from the known weight percentages of water and maltose in the samples. For example, in an 80 wt % maltose sample, the ratio of water to maltose molecules is 4.75 and thus the ratio B/A is calculated to be 9.5:22 = 0.43. As is seen in Fig. 2, this value is reached at a temperature of 248 K (see Table 1). The results for the various maltose-water samples are summarized in Table 1. In this table, it can be noticed that the temperature at which the calculated ratio B/A (($B/A)_{calc}$) is observed (indicated by the dashed horizontal lines in Fig. 2), tends to follow the glass transition temperature T_g. At higher or lower temperatures, the ratio B/A deviates from $(B/A)_{calc}$. This occurs because the separation of the NMR signal by the fit procedure is not based on discrimination between maltose and water protons but on discrimination between mobile and immobile protons. This separation is temperature dependent because the molecular mobility is

wt% maltose	water/maltose	$(B/A)_{calc}$	T_{calc} (K)	T_g (K)
80	4.75	0.43	248	242
90	2.11	0.19	269	278
93	1.43	0.13	297	292
95	1.00	0.09	300	297

Table 1 The molecular ratio of water and maltose, the calculated ratio B/A (B/A)calc based on proton densities of water and maltose, the temperature (Tcalc) where this value of B/A is measured, and the glass transition temperature (Tg) for various maltose-water samples.

temperature dependent. Therefore, it is possible that we find that above T_g more 'mobile' protons exist than we can account for on basis of the known water content, whereas below T_g we find less 'mobile' protons than we can account for.

A higher than calculated value of the ratio B/A can be explained by maltose protons becoming mobile, although it has also been explained to arise from chemical exchange between the water and the maltose protons. Chemical exchange is exchange of protons of the water and the sugar by which magnetization is exchanged [25, 26]. If chemical exchange times have the same time scale as T_{2m}, 10^{-5} s, this exchange can significantly influence the amplitudes of the mobile and immobile fractions. Although it was observed[27] that the chemical exchange time for 60 wt % glucose water samples at room temperature is on the order of 10^{-2} s, and thus too slow to influence the ratio B/A, we also measured cross relaxation rates to estimate the influence of the chemical exchange rate on the ratio B/A in 80-95 wt % maltose-water samples at low temperatures. Cross relaxation is the inter and intramolecular transfer of magnetisation of protons by chemical exchange and/or spin diffusion. These effects can be measured with the Goldman Shen pulse sequence[17, 18]. In this pulse sequence, the difference in transverse relaxation between the immobile and the mobile protons is used to determine the cross relaxation between the mobile and immobile protons. The cross relaxation rate in maltose glasses decreases with temperature and water content because the more rigid a sample, the more efficient is the cross relaxation takes place (data not shown). For the temperature and water content range we used, the cross relaxation rate was on the order of 10^3 s^{-1}, which is similar to the value observed before[11]. The upper limit for chemical exchange rate is thus 10^3 s^{-1} while the transverse relaxation rates are at least 50 times larger (Fig. 3). Thus, chemical exchange is too slow to influence the amplitudes B and A. The higher than calculated value

of the ratio B/A above T_g must therefore be explained by sugar protons becoming mobile.

Most likely, the exocyclic hydroxyl protons of the sugar first go over from the immobile to the mobile fraction when the temperature is increased, because they are most remote to the ring and have therefore a higher, albeit restricted, mobility. If for example, the two exocyclic hydroxyl protons go over to fraction B in a 80 wt % maltose sample, the ratio B/A is 0.57, which is reached at 25 degrees above T_g. Within the temperature and water content range we studied, two to three sugar protons at most behave in a liquid-like way. As mentioned above, in previous studies it was suggested that the hydroxyl protons of sugar molecules could contribute to the mobile protons in ^{1}H NMR experiments via chemical exchange.[21-23, 28] However, the hydroxyl protons contribute to the mobile fraction because these protons become mobile not because of chemical exchange. At temperatures below T_g, the contribution of the immobile protons is relatively too large, which means that some water protons are immobile. This is illustrated by the fact that in 80 wt % maltose, the ratio B/A is 0.18 in the case that half of the water protons are immobile. This point is reached at 220 K. Solid water protons were also observed in 93 wt % starch at low temperatures [24].

The slope of B/A versus temperature is a measure of the amount of protons going over from the immobile to the mobile fraction per degree (Fig. 2). Below T_g the slope reflects the water protons becoming mobile. The slope of B/A versus temperature increases with water content, because the more water protons are present the more protons will become mobile per degree of temperature. The slope of B/A in a sample with 20 wt % water is therefore expected to be 4.75 times higher than in a sample with 5 wt % water. The increase in mobility of the protons with temperature is a gradual process, and T_g

T	A (immobile)	B (mobile)
$< T_g$	maltose + H_2O	H_2O
T_g	maltose	H_2O
$> T_g$	maltose	H_2O + maltose

Table 2 The temperature dependent assignment of the mobile (B) and immobile (A) fraction in terms of water and sugar.

is not marked by any discontinuity or a change in the rate of this process (Fig. 2). However above T_g, where all water protons already are mobile, the slope reflects the OH groups of the sugar becoming so mobile that they no longer belong to the solid fraction. The amount of maltose protons decreases with increasing water content, but the slope above T_g increases with water content. This indicates that the average maltose proton mobility is higher in a sample with 20 wt % water as compared to a sample with 5 wt % water.

By a linear extrapolation to lower temperatures, the ratio B/A becomes zero around 200 K. This means that then no water mobility would be observed by ^{1}H NMR. In cellulose, in which the water molecules have a similar molecular environment, it was also observed that water mobility vanishes around 190 K [29]. Only a highly mobile independent flipping of some water molecules still persisted. Water mobility observed with ^{1}H NMR in organic polymers also vanishes in the same temperature range (160 - 190 K). [30-33]

The temperature dependent assignment of the mobile and immobile fraction to water and maltose protons is summarized in Table 2. Below T_g, the mobile fraction (on the average) is thought to consist of only water protons. It is important for the following discussion to keep in mind that the immobile fraction

at temperatures below T_g consists of water and sugar protons and that at higher temperatures both sugar and water contribute to the mobile fraction.

In Fig. 3, it can be seen that in all samples the transversal relaxation time T_{2m} of the mobile fraction increases with increasing temperature. A small break in T_{2m} is observed at the glass transition temperature T_g. This indicates an additional increase in reorientational motions of the mobile water protons at T_g. From the dependence on water content, it can be seen that the fewer water molecules per maltose molecule, the stronger the water molecules sense the glass transition. This shows that at lower water contents the water molecules tend to have stronger interactions with the maltose molecules. The value of T_{2m} of about 10^{-4} s in maltose samples around T_g is a factor of 10^5 smaller than the T_2 of free water. The value of τ_c of water in maltose glasses is thus expected to be 10^{-7} s. This observation illustrates that water mobility is decoupled from the viscosity of the sample, which increases by a factor of 10^{12}, while the rotational mobility of the water is only slowed down by a factor of 10^5. This decoupling of mobility of small molecules from the matrix mobility has been observed before in a glassy matrix [9, 13, 34-36]. In epoxy-resin [37, 38] or poly(vinylpyrrolidone)[16] glasses, water mobility is even less retarded compared to free water, probably because these polymers are much more hydrophobic and cannot form multiple hydrogen bonds. Not only rotational mobility but also translational mobility of small molecules is decoupled from the matrix mobility[13, 15, 39, 40]. In Ficoll, a sucrose based polymer, the translational mobility of water as determined from desorption experiments is unaffected by the glass transition of the carbohydrate [15]. The translational mobility of water was also found to be decoupled by a factor of 10^7 from that of the carbohydrate matrix in concentrated maltose samples in the vicinity of T_g [13, 40].

On comparing T_{2m} at the glass transition temperatures of every water content, it can be seen that T_{2m} increases with increasing water content. The value of T_{2m} depends on dipole interactions and rotational mobility. The dipole interactions of water protons are mainly determined by the distance of the two protons of water and thus constant. Therefore it follows that at T_g the water molecules in an 80 wt % maltose-water sample are more mobile as compared to water molecules in a 95 wt % maltose-water sample, even though the temperature T_g has decreased. Theoretically, T_{2m} increases with temperature by an increase in molecular mobility. Therefore a lower value of T_{2m} is expected at a lower glass transition temperature T_g. Such an effect is observed, for example, in a series of malto-oligomer samples with constant water content in which the chain length is varied[9]. However, for our maltose-water samples, this is not the case, and it can be concluded that the effect of water content on the rotational mobility exceeds the effect of temperature.

Clearly, increasing the water content reduces the molecular interactions between water and maltose protons and thus increases the rotational mobility. It is likely that in these highly concentrated maltose-water samples the water molecules mostly interact with the hydroxyl groups of the sugar [41]. A water molecule in a 95 wt % maltose sample hardly interacts with other water molecules in the time that the NMR signal decays. This can be calculated from the equation $x = \sqrt{2Dt}$, in which x is the displacement and t the time. The diffusion coefficient D is 10^{-14} m^2/s in a 95 wt % sample at its glass transition temperature [13, 40]. In such a maltose sample, having only one water molecule per maltose molecule, the calculated displacement of a water molecule (0.5 nm) during the time the NMR signal decays (around 10^{-5} s, the value of T_2), is on the same order of magnitude as the size of a maltose molecule. Thus, the water molecules in a 95 wt % maltose sample do not interact with other water molecules but will only form hydrogen bonds with maltose hydroxyl protons. On

44

increasing the water content, more hydrogen bonds are formed between the water molecules, and this leads to an increase in motion and thus longer T_{2m} values. From the relaxation behavior of the mobile protons, it can be concluded that the rotational motion of the water molecules is decoupled from the mobility of the maltose molecules, as expected. However, at low water contents, the water molecules strongly interact with the maltose molecules and therefore sense the glass transition.

Having discussed the relaxation of the mobile protons, we proceed with the discussion of the immobile protons. The part of the FID originating from the immobile protons cannot be characterized by a T_2 value, and therefore the method of second moments is used[19]. This method was employed already in earlier studies of mobility in crystalline sugars[42, 43] and glucose penta acetate[44].

The variation of the second moment M_2 of the immobile protons with temperature is shown in Fig. 4. In the analysis of M_2, the following points should be taken into account:

1. A reduction of M_2 takes place if the proton density in the sample is lowered, because dipolar interactions decrease with the sixth power of the distance between protons.

2. M_2 will be reduced by anisotropic mobility or slow isotropic rotations that partly average out the dipolar interactions.

A clear indication for the first effect is seen on comparing the deuterated and protonated maltose-water samples. Since the average distance between the protons increases in the deuterated samples and deuterons hardly contribute to the dipolar couplings because of their low gyromagnetic ratio, the second moment M_2 is reduced in deuterated samples. Furthermore, the increasing

45

value of M_2 below T_g is explained by an increasing proton density, because the relative number of protons contributing to M_2 is increasing. Also, the temperature dependence of M_2 is related to effect 1. From Fig. 2, we concluded that upon decreasing the temperature below T_g more and more water protons become part of the immobile fraction. These protons increase the value of M_2 because they give rise to an increased static proton density and a concomitant decrease in apparent proton-proton distances. The more water protons that become immobile, the stronger the increase in M_2. Therefore the slope of M_2 versus temperature is larger for 80 wt % maltose-water samples as compared to 95 wt % maltose-water samples below T_g.

Related to the amount of immobile water protons is the limiting value of M_2 that is reached at low temperatures, where all water protons are immobilized. This limiting value should be higher in a 80 wt % maltose-water sample than in a 95 wt % sample, because the effect of water is to reduce the proton-proton distances, and thus to increase M_2. Although this limiting value is not reached in the temperature range studied, the higher values of M_2 in a 80 wt % maltose-water sample as compared to a 95 wt % sample support this reasoning (Fig. 4). The value of M_2 around T_g in a 95 wt % maltose-water sample (1.15×10^{10} s^{-2}) is somewhat smaller than the value of M_2 in monohydrate crystalline maltose (1.23×10^{10} s^{-2})[42] calculated from the known X-ray structure[45]. The somewhat lower experimental value of M_2 may reflect some local motions of the water molecules[42] (effect 2).

On increasing the temperature, all protonated maltose-water samples show a break in M_2 just above T_g. This relatively steep decrease of M_2 cannot be explained by proton density arguments, because Fig. 2 shows no discontinuities around T_g. Therefore, the increase in slope just above T_g must be explained by the onset of additional mobility of hydroxyl or non-

46

exchangeable protons (effect 2) that reduces M_2 more strongly than was the case below T_g. In the deuterated samples, this discontinuity is not observed above T_g, but below T_g. Thus, the extra decrease of M_2 above T_g in protonated samples is not due to extra mobility of the non-exchangeable maltose protons but to mobility of hydroxy protons. The steep decrease in M_2 displayed by the deuterated samples does not coincide with T_g nor with the temperatures reported for β-relaxation (203 K for 80 wt % and 219 K for 93 wt % maltose samples [7]). This effect can be explained as follows. Starting at low temperature, the motion of the non-exchangeable protons will gradually increase on increasing the temperature. However, at low temperatures the anisotropic mobility of these protons is too slow to influence M_2. This is reflected in the horizontal plateau value of M_2. At a certain temperature, the motions start to reduce M_2, giving rise to the observed decrease. This temperature is not necessarily related to T_g. It is likely that at first instance the decrease will probably be due to librations of the protons of the exocyclic CH_2OD groups, because they are most remote to the ring and therefore have an additional degree of motional freedom. It should be noted, however, that the effect of the non-exchangeable groups will play a role in the protonated samples, but it is overshadowed by the relatively large contribution of the exchangeable hydroxyl protons.

On the basis of the M_2 results, we can conclude that around T_g the hydroxyl protons of the maltose molecules become mobile. This suggests that the hydrogen-bond network starts to 'melt' at T_g. A similar effect was deduced from molecular dynamics simulations [46, 47]. Here T_g is found to indicate an abrupt change in the hydrogen-bond properties (lifetime times number of hydrogen bonds), and upon heating, a weakening of the hydrogen-bond network is observed. Also neutron-scattering experiments with glassy glucose showed that

47

the hydrogen network becomes less pronounced on heating, and that the glass transition is accompanied by a decrease in the number of hydrogen bonds[48].

The mobility of the hydroxyl protons also explains why the value of M_2 at T_g decreases with water content. The value of M_2 is higher for a protonated 93 wt% maltose-water sample as compared to a 80 wt % sample, while in deuterated samples there is no such difference in M_2 at T_g. Therefore, the decrease of M_2 at T_g with increasing water content must be due to mobility of the water or hydroxyl protons. Because at T_g all water protons belong to the mobile fraction (Table 2), we conclude that the lower value of M_2 at T_g with increasing water content is due to more mobile hydroxyl protons. Thus, the main effect of adding water is not an increase of water mobility but its effect on the maltose. The presence of water enhances the mobility of hydroxyl protons of maltose. If the mobility of the glass-forming molecules is large, the sample has to be cooled to a lower temperature before a glass is formed. This plasticization mechanism is similar to that in polymer glasses where plasticizers increase the mobility of side chains of the polymer. Water in poly(vinyl alcohol) is said to provide a lubrication effect that promotes chain mobility and disrupts hydrogen bonding, removing further barriers to bond rotation and chain mobility [49].

On the basis of our results, we propose the following model for the molecular mobility in low water content maltose-water samples. The mobility of water and maltose protons decreases with decreasing water content and temperature. The glass transition is marked by a decrease in the temperature dependence of mobility of the hydroxyl protons of maltose. As a result of strong interactions between the maltose and water protons at low water contents, the water molecules also sense the glass transition. This suggests that upon cooling a stable hydrogen-bond network between the sugar molecules is formed at the

48

glass transition temperature, which immobilizes the hydroxyl groups. Water molecules weaken this network, which results in a higher mobility of the hydroxyl protons of maltose. The more water, the stronger this plasticizing effect. This property of water also explains why samples with a higher water content have to be cooled to lower temperatures before a glass is formed.

ACKNOWLEDGMENTS

REFERENCES

1. Y. Roos *Phase Transitions in Foods*; Academic Press: San Diego, 1995.

2. M. J. G. W. Roozen, M. A. Hemminga and P. Walstra. *Carbohydr. Res.* **1991**, *215*, 229-237.

3. M. J. G. W. Roozen and M. A. Hemminga. *Spec. Publ. - R. Soc. Chem.* **1991**, *82*, 531-536.

4. M. J. G. W. Roozen and M. A. Hemminga. *J. Phys. Chem.* **1990**, *94*, 7326-7329.

5. M. T. Cicerone, F. R. Blackburn and M. D. Ediger. *Macromolecules* **1995**, *28*, 8224-8232.

6. M. T. Cicerone and M. D. Ediger. *J. Chem. Phys.* **1996**, *104*, 7210-7218.

7. T. R. Noel, R. Parker and S. G. Ring. *Carbohydr. Res.* **1996**, *282*, 193-206.

8. R. M. Diehl, F. Fujara and H. Sillescu. *Europhys. Lett.* **1990**, *13*, 257-62.

9. S. Ablett, A. H. Darke, M. J. Izzard and P. J. Lillford *Studies of the glass transition in malto-oligomers*; Nottingham University Press: Nottingham, 1993.

10. D. Girlich, H. D. Lüdemann, C. Buttersack and K. Buchholz. *Z. Naturforsch. C* **1994**, *49*, 696.

11. B. P. Hills and K. Pardoe. *Journal of Molecular Liquids* **1995**, *63*, 229-237.

12. M. D. Ediger, C. A. Angell and S. R. Nagel. *J. Phys. Chem.* **1996**, *100*, 13200-13212.

13. R. Parker and S. G. Ring. *Carbohydr. Res.* **1995**, *273*, 147-55.

14. D. Girlich and H.-D. Lüdemann. *Z. Naturforsch.* **1993**, *49*, 250-257.

15. B. J. Aldous, F. Franks and A. L. Greer. *J. Mat. Sc.* **1997**, *32*, 301-308.

16. C. A. Oksanen and G. Zografi. *Pharm. Res.* **1993**, *10*, 791-9.

17. A. M. Kenwright and K. J. Packer. *Chem. Phys. Lett.* **1990**, *173*, 471-475.

18. M. Goldman and L. Shen. *Phys. Rev.* **1966**, *144*, 321-331.

19. A. Abragam *The principles of nuclear magnetism*; Clarendon Press: Oxford, 1961.

20. V. J. McBrierty and K. J. Packer *Nuclear magnetic resonance in solid polymers*; Cam. Univ. Press: Cambridge, 1995.

21. M. T. Kalichevsky, E. M. Jaroszkiewicz, S. Ablett, J. M. V. Blanshard and P. J. Lillford. *Carbohydrate Polymers* **1992**, *18*, 77-88.

22. M. T. Kalichevsky, E. M. Jaroszkiewicz and J. M. V. Blanshard. *Polymer* **1993**, *34*, 346-58.

23. I. A. Farhat, J. R. Mitchell, J. M. V. Blanshard and W. Derbyshire. *Carbohydrate Polymers* **1996**, *30*, 219-227.

24. S. Li, L. C. Dickinson and P. Chinachoti. *J. Agric. Food Chem.* **1998**, *46*, 62-71.

25. H. T. Edzes and E. T. Samulski. *J. Magn. Res.* **1978**, *31*, 207-229.

26. J. R. Zimmerman and W. E. Brittin. *J. Phys. Chem.* **1957**, *61*, 1328-1333.

27. B. P. Hills. *Molecular Physics* **1991**, *72*, 1099-1121.

28. S. Ablett, M. J. Izzard and P. J. Lillford. *J. Chem. Soc. Far. Trans.* **1992**, *88*, 789-794.

29. D. Radloff, C. Böffel and H. W. Spiess. *Macromolecules* **1996**, *29*, 1528-1534.

30. F. M. Coyle, S. J. Martin and V. J. McBrierty. *Journal of Molecular Liquids* **1996**, *69*, 95-116.

31. V. J. McBrierty, X. Zhang, D. C. Douglass, J. X. Zhang and R. Jerome. *Polymer* **1994**, *35*, 3811-3815.

32. F. X. Quinn, E. Kampff, G. Smyth and V. J. McBrierty. *Macromolecules* **1988**, *21*, 3191-3198.

33. G. Smyth, F. X. Quinn and V. J. McBrierty. *Macromolecules* **1988**, *21*, 3198-3204.

34. F. R. Blackburn, M. T. Cicerone, G. Hietpas, P. A. Wagner and M. D. Ediger. *J. Non-Cryst. Sol.* **1994**, *172*, 256-264.

35. F. R. Blackburn, C. Wang and M. D. Ediger. *J. Phys. Chem.* **1996**, *100*, 18249-18257.

36. I. Chang, F. Fujara, B. Geil, G. Heuberger, T. Mangel and H. Sillescu. *Journal of Non - Crystalline Solids* **1994**, *172*, 248-255.

37. L. W. Jelinski, J. J. Dumais, A. L. Cholli, T. S. Ellis and F. E. Karasz. *Macromol.* **1985**, *18*, 1091-1095.

38. L. W. Jelinski, J. J. Dumais, R. E. Stark, T. S. Ellis and F. E. Karasz. *Macromol.* **1983**, *16*, 1019-1021.

39. D. Champion, H. Hervet, G. Blond, M. Le Meste and D. Simatos. *J. Phys. Chem. B* **1997**, *101*, 10674-9.

40. R. H. Tromp, R. Parker and S. G. Ring. *Carbohydr. Res.* **1997**, *303*, 199-205.

41. D. Girlich and H.-D. Lüdemann. *Z. Naturforsch.* **1993**, *48c*, 407-413.

42. E. C. Reynhardt. *Mol. Phys* **1990**, *69*, 1083-97.

43. E. C. Reynhardt and L. Latanowicz. *Chemical Physics Letters* **1996**, *251*, 235-241.

44. B. Ellis and M. P. McDonald. *J. Non-Cryst. Solids* **1969**, *1*, 186-94.

45. M. E. Gress and G. A. Jeffrey. *Act. Cryst.* **1977**, *B33*, 2490-2495.

46. E. Caffarena and J. R. Grigera. *J. Chem. Soc. Faraday Trans.* **1996**, *92*, 2285-2289.

47. E. R. Caffarena and J. R. Grigera. *Carbohydrate Research* **1997**, *300*, 51-57.

48. R. H. Tromp, R. Parker and S. G. Ring. *Journal Of Chemical Physics* **1997**, *107*, 6038-6049.

49. R. M. Hodge, T. J. Bastow, G. H. Edward, G. P. Simon and A. J. Hill. *Macromolecules* **1996**, *29*, 8137-8143.

4

Effects of water content and molecular weight on spin probe and water mobility in malto-oligomer glasses

Ivon van den Dries, Dagmar van Dusschoten, Marcus Hemminga and Erik van der Linden

ABSTRACT

Spin probe rotational mobility has been studied by means of saturation transfer ESR in malto-oligomer-water glasses and has been compared to water mobility as measured by ^{1}H-NMR. Increasing the water content from 10 to 30 wt % leads to a decrease in spin probe mobility at T_g while the water mobility increases at T_g. From FTIR data we conclude that this decrease in spin probe mobility is caused by the fact that the overall packing of water and carbohydrate molecules in the hydrogen bonded network becomes denser upon increasing water content. From proton density measurements we conclude that the concomitant increase in mobility of water molecules is caused by the fact that the carbohydrate molecules become more separated from one another. Both water and spin probe mobility at T_g increase upon increasing the molecular weight of the malto-oligomers (ranging from glucose up to maltoheptaose), while keeping the water content constant. This can be explained by the fact that larger oligomers form less densely packed networks.

INTRODUCTION

Glasses of carbohydrates play an important role in the preservation and storage of foods[1], pharmaceutical products[2, 3] and seeds[4] due to the very low molecular mobility in these carbohydrate glasses. The molecular mobility in carbohydrate glasses affects characteristics such as stickiness, collapse, reaction rates of enzymatic reactions, the evaporation of volatile flavors, and hydration/dehydration processes. Usually carbohydrate glasses contain some water, which acts as a plasticizer, decreasing the glass transition temperature (T_g). Water is an important factor determining the chemical and physical stability of glasses[3, 5-8], since it affects their structure.

Relatively small amounts of water reduce the glass transition temperature dramatically. E.g. the glass transition temperature of maltose drops from 353 K to 241 K upon the addition of 20 wt % water [8]. This phenomenon is referred to as plasticization and is usually related to weakening or rupturing of the interaction between matrix molecules and their replacement by a weaker plasticizer-matrix molecule interaction[9]. For a molecule to be effective as a plasticizer the intermolecular forces in the plasticizer and the matrix must be alike[9], as is the case in water and sugar because both form hydrogen bonded networks. From positron annihilation studies it is known that the addition of a plasticizer can have several effects on the free volume between the matrix molecules[9-16]. On the one hand, plasticizer molecules can fill up voids between the matrix molecules and thereby they can lower the free volume. On the other hand, addition of plasticisers can also lead to an increase in free volume by decreasing the molecular packing of the matrix molecules, which occurs e.g. during swelling of a polymer[11, 12, 14, 17, 18].

In order to determine the structural effects of water and molecular weight of oligomers in oligomer-water glasses we studied the molecular mobility in carbohydrate-water mixtures around the glass transition temperature. In particular we choose to study water and spin probe rotational mobility. Water rotational mobility is studied by the relaxation behavior of the mobile protons (T_{2m}) in proton Nuclear Magnetic Resonance (^{1}H-NMR) experiments[19]. Spin probe rotational mobility is measured with electron spin resonance (ESR) techniques and characterized by a rotational correlation time, τ_R. The value of τ_R around T_g lies in the range of 10^{-4} to 10^{-2} s and is therefore measured using Saturation Transfer Electron Spin Resonance techniques (ST-ESR).

Both water and spin probe mobility were studied as a function of water content in glucose and maltose glasses, and as a function of the molecular weight of the malto-oligomers (1-7 monomers). Additional structural information about the average distance between sugar molecules was obtained using proton density determination from ^{1}H-NMR experiments. the strength of the hydrogen bonded network was obtained from the OH stretch vibration using Fourier transform infrared spectroscopy (FTIR).

MATERIALS AND METHODS

Preparation of samples

Sugar glasses were prepared in two ways.1) The appropriate amounts of sugar and water were mixed, melted, and quickly cooled below the glass transition temperature (T_g) to obtain concentrated sugar-water glasses. The water contents of the glucose samples and the corresponding T_g values, taken from DSC data of Noel et al. [8], are 68 wt % (T_g = 191), 73 (201), 78 (213), 79 (215), 81 (223), 85 (233), and 89 wt % (247) and for maltose-water samples 71 wt % (T_g = 215), 72 (219), 78 (234), 80 (241), 81 (245), and 87 (261), respectively. 2)

Alternatively, upon cooling aqueous solutions of sugars (20 wt %) ice is formed and thereby the remaining sugar solution is concentrated up to approximately 80 wt % sugar, forming freeze concentrated glasses. Anhydrous glucose was obtained from Jansen Chimica, glucose monohydrate and maltose monohydrate from Merck, and the malto-oligosaccharides were obtained from Sigma. The sugar concentration in the ESR samples was adjusted with water and an aqueous solution of the spin probe 4-hydroxy-2,2,6,6-tetramethylpiperidine N-oxyl (TEMPOL, obtained from Sigma). The final concentration of the TEMPOL spin probe in the samples was 0.2 - 0.5 mg/ml. Anhydrous glycerol used to calibrate the ESR spectra was obtained by mixing glycerol with the spin probe solution and dried over phosphorpentoxide under vacuum for at least two weeks. For the use in ESR and ST-ESR experiments, the samples were sealed in 100 µl tubes (Brandt). The sample height was 5 mm. For the NMR samples appropriate amounts of sugar and water were mixed in 5 mm NMR tubes and sealed to prevent water evaporation. Both ESR and NMR samples with a sugar concentration above 60 wt % were melted quickly at temperatures as low as possible to obtain a homogeneous sample without browning and without degradation of TEMPOL. Melted samples were quickly cooled and stored below their respective glass transition temperatures. In order to obtain deuterated NMR samples the sugars were dissolved in D_2O and freeze-dried. This procedure was repeated to complete the exchange of the hydroxyl protons before adjusting the water content with D_2O. FTIR samples were prepared by rapid drying of 10 µl of a sugar solution (20 wt %) on circular CaF_2 (13 X 2 mm diameter) windows in a cabin that was continuously purged with dry air (relative humidity < 3% at 297 K). Rehydration of sugar glasses was achieved by placing the windows containing the glasses for 2 days in closed boxes at different relative humidities (RH), established by saturated salt solutions (RH=13% and 33% for LiCl and $MgCl_2$ solutions, respectively)[20].

ESR Spectroscopy

ESR and ST-ESR spectra were recorded on a Bruker ESR spectrometer ESP 300E equipped with a TMH (Bruker) cavity and nitrogen temperature control. The sample capillaries were placed in 4 mm quartz ESR sample tubes and carefully placed in the center of the microwave cavity. The temperature was measured with a small CuCo thermocouple close to the sample. The temperature stability is ±1.0 K. All samples were rapidly cooled to a temperature between 140-180 K and subsequently measured during stepwise warming up. For conventional ESR the microwave power was set to 2 mW. The scan range, scan rate, time constant, and field modulation amplitude were adjusted so that distortion of the spectra was avoided. For ST-ESR spectroscopy the second harmonic quadrature absorption signal was detected under the following conditions;[21, 22] field modulation amplitude 0.5 mT, microwave power 100 mW, and field modulation frequency 50 kHz. The phase was set with the self-null method [23]. Data analysis to obtain the rotational correlation times of TEMPOL was carried out as described previously [24].

FTIR spectroscopy

Infrared absorption measurements were carried out with a Perkin-Elmer series 1725 Fourier transform infrared spectroscope equipped with an external beam facility to which a Perkin-Elmer IR microscope was attached. The microscope was equipped with a narrow band Mercury/Cadmium/Telluride liquid nitrogen-cooled IR-detector. The temperature was regulated with a nitrogen temperature control and the temperature was measured close to the sample windows. The temperature dependence of the IR spectra was studied while warming the sample with a scanning rate of 1-1.5 K/min. The optical bench was purged with dry CO_2-free air (Balston; Maidstone, Kent, UK) at a flow rate of 25 L/min. The acquisition parameters were: 4 cm^{-1} resolution, 32 added interferograms, 3500-900 cm^{-1} wavenumber range. The peak position of the OH-stretching

57

band in the spectral region between 3500 and 3000 cm $^{-1}$ was calculated as the average of the spectral positions at 80% of the peak height. T_g was determined as the intersection point of two lines obtained by linear regression of the wavenumber of the OH-stretching bands as a function of temperature below and above T_g, respectively [20].

¹H-NMR spectroscopy

¹H NMR measurements were performed on a Bruker AMX 300 spectrometer equipped with a Bruker 5 mm proton probe operating at a resonance frequency of 300.13 MHz. The temperature was regulated with a nitrogen temperature control. In this way, the temperature stability was within ±0.5 K. A spectral width of 500 kHz was used. The duration of the 90° pulse was 6-7 µs. The presented free induction decays (FID) are averages of 128 or 256 scans having 2048 data points. For the analysis of the NMR, the FIDs F(t) were fitted to the following equation[19]:

$$F(t) = A \exp\left[\frac{-a^2 t^2}{2}\right] \frac{\sin bt}{bt} + B \exp\left[\frac{-t}{T_{2m}}\right] \tag{1}$$

In this equation, the parameters A and B represent the contributions of the immobile and mobile protons, while T_{2m} denotes the spin-spin relaxation time of the mobile proton fraction. The NMR spectrum of the immobile proton fraction is assumed to be a rectangular line shape with a total width 2b, convoluted with a Gaussian line shape with a standard deviation given by parameter a [19,20]. The second moment M_2 of the broad line shape, which is a measure of the strength of the dipolar interactions, is given by [19]

$$M_2 = a^2 + \frac{1}{3} b^2 \tag{2}$$

DSC

Samples with a weight between 10 and 20 mg were measured using a Pyris 1
DSC (Perkin-Elmer) at cooling and heating rate of 10 K/min. From the heating
scans the onset of the glass transition T_g' and of ice melting T_m' were
determined. For maltopentaose-, maltohexaose- and maltoheptaose-water
samples the glass transition cannot be distinguished from the melting of ice and
therefore only one transition temperature is reported.

RESULTS

Rotational correlation times of TEMPOL in concentrated and freeze
concentrated glasses are shown in Fig. 1 as a function of temperature. No data
points are gathered in the range $10^{-8} < \tau_R < 10^{-6}$ s since this range is not well-
accessible by means of the two techniques used (conventional ESR and ST
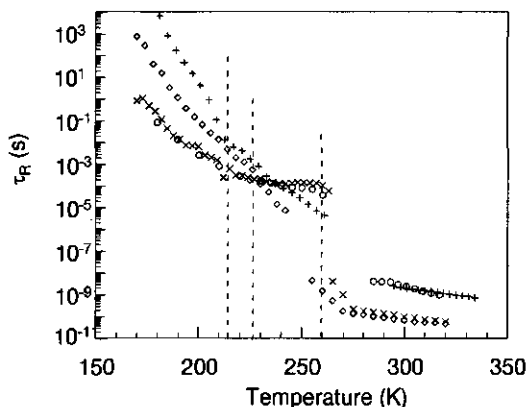ESR). For freeze concentrated glasses the glass transition temperature, T_g',

Figure 1 Rotational correlation times τ_R of TEMPOL in concentrated (80 wt %) glucose
(+) and maltoheptaose (o) and in freeze concentrated glucose (◊) and maltoheptaose (x)
as a function of temperature. Dotted lines indicate T_m' (glucose: 227 K, maltoheptaose:
260), T_g' (glucose: 212 K, maltoheptaose: 260) , and T_g (glucose: 212 K, maltoheptaose:
260 K).

wt % of malto-oligomers	M_n (g)	T_g' (K)	T_m' (K)	T_m'ESR (K)	τ_R (T_g') (s)	τ_R (T_m') (s)	E_{act} (kJ/mol)
20 glucose	64.3	212	227	225	$7.6\ 10^{-3}$	$3.1\ 10^{-4}$	82.4
17.5 glucose + 2.5 maltoheptaose	66.3	210	230	224	$3.7\ 10^{-3}$	$3.1\ 10^{-4}$	83.4
15 glucose + 5 maltoheptaose	68.5	210	233	225	$1.3\ 10^{-2}$	$5.6\ 10^{-4}$	81.3
12.5 glucose +7.5 maltoheptaose	70.7	213	234	231	$3.5\ 10^{-3}$	$2.2\ 10^{-4}$	56.3
10 glucose +10 maltopentaose	72.4	214	237		$9.0\ 10^{-3}$		48.4
10 glucose +10 maltoheptaose	73.2	215	238	237	$2.5\ 10^{-3}$	$1.7\ 10^{-4}$	45.6
20 maltose	75.0	227	242	238	$7.4\ 10^{-4}$	$1.0\ 10^{-4}$	51.8
15 maltose + 5 maltoheptaose	77.3	226	245	241	$3.7\ 10^{-4}$	$7.3\ 10^{-5}$	44.8
10 maltose +10 maltopentaose	78.3	231	248	246	$2.0\ 10^{-4}$	$5.5\ 10^{-5}$	46.9
15 maltoheptaose +5 glucose	78.6		247	241		$5.8\ 10^{-5}$	53.6
20 maltotriose	78.8	237	249	245	$1.5\ 10^{-4}$	$7.1\ 10^{-5}$	47.2
10 maltose +10 maltoheptaose	79.6	230	249	245	$3.2\ 10^{-4}$	$4.7\ 10^{-5}$	34.7
15 maltotriose + 5 maltoheptaose	80.2	237	251	246	$1.2\ 10^{-4}$	$5.8\ 10^{-5}$	41.3
20 maltotetraose	81.2	245	253	250	$9.1\ 10^{-5}$	$5.3\ 10^{-5}$	41.2
17.4 maltoheptaose + 2.6 glucose	81.6	253	253		$5.9\ 10^{-5}$		48.4
10 maltotriose +10 maltoheptaose	81.7	237	254	249	$1.3\ 10^{-4}$	$5.3\ 10^{-5}$	40.6
15 maltoheptaose + 5 maltose	82.1	253	253	246	$3.8\ 10^{-5}$		39.5
20 maltopentaose	82.8	256	256	255	$6.7\ 10^{-5}$		40.5
15 maltoheptaose + 5 maltotriose	83.2	240	257	250	$9.5\ 10^{-5}$	$3.4\ 10^{-5}$	38.9
17.5 maltoheptaose + 2.5 maltose	83.4	257	257		$5.0\ 10^{-5}$		30.5
20 maltohexaose	83.9	258	258	255	$5.3\ 10^{-5}$		36.9
19.5 maltoheptaose +0.5 glucose	84.1	258	258	252	$5.3\ 10^{-5}$		46.7
20 maltoheptaose	84.7	260	260	255	$3.8\ 10^{-5}$		37.0

Table 1 The onset of ice melting (T_m') and the glass transition temperature (T_g') result from DSC measurements and the onset of ice melting (T_m'ESR), the values of apparent activation energy for rotation below T_g' (E_{act}) and the rotational correlation times of TEMPOL at T_g' (τ_R (T_g')) and T_m' (τ_R (T_m')) result from ESR experiments in freeze concentrated mixtures of oligomers with increasing number average molecular weight (M_n). The total sugar concentration is 20 wt % and the numbers in the first column indicate the weight percentage of each compound.

and the melting temperature, T_m', were obtained from DSC experiments (Table 1). For concentrated glasses the T_g values are taken from Noel et al. [8]. The T_g' values correspond with the T_g values of 80 wt % glasses indicating that the freeze concentration is 80 wt % The value of T_m' can also be obtained from Fig. 1 because it is marked by an abrupt change in slope at τ_R at 227 K for glucose and 259 K for maltoheptaose, respectively. The stronger increase in τ_R above this discontinuity is due to the melting of ice and subsequent dilution of the spin probe environment. The melting temperature as obtained from the discontinuity is 1 to 7 K lower than T_m' as obtained with DSC (Table 1).
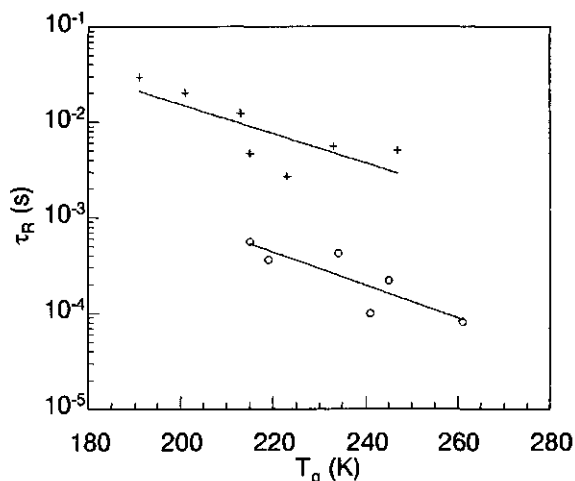

Figure 2 Rotational correlation times at the glass transition temperature τ_R (T_g) of TEMPOL in concentrated glucose (+) and maltose (o) glasses as function of T_g.

Effect of water content

The effect of water on spin probe mobility at the respective glass transition temperatures is compared in glucose and maltose glasses. The value of τ_R at the glass transition temperature ($\tau_R(T_g)$) of concentrated glucose and maltose systems is found to decrease with increasing T_g values (Fig. 2). In other words,

the spin probe mobility in glucose and maltose glasses at their respective glass transition temperatures is decreased upon increasing water content.

The spin probe mobility in glucose and maltose glasses is compared to the mobility of the water protons as measured with ^{1}H- NMR. In Fig. 3 the relaxation time of the mobile fraction of protons (T_{2m}) shows an increase with temperature and water content. $T_{2m}(T_g)$ is proportional to water rotational mobility. This is because T_{2m} is in general proportional to rotational mobility if
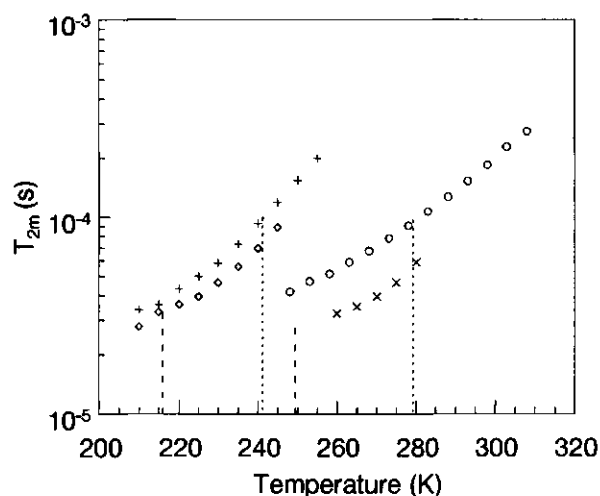

Figure 3 The transverse relaxation time of the mobile protons (T_{2m}) in 80 wt % ($\Diamond$) and 90 wt % (x) glucose-water and in 80 wt % (+) and 90 wt % (o) maltose-water mixtures around T_g indicated with lines for glucose (——) and maltose (.....) .

$1/\tau_R \ll$ Larmor frequency (according to the Blumbergen-Purcell-Pound theory[25]), and because at T_g all protons in the mobile fraction are water protons. The fact that all mobile protons are water protons follows from the ratio of amplitudes of the mobile and immobile component in the FID (B/A). If this value at T_g is smaller than the theoretical B/A value as calculated by assuming all water protons mobile and all sugar protons immobile, it is concluded that all mobile protons are water protons[19]. In 80 and 90 wt % maltose and 80 wt %

glucose B/A at T_g is smaller than the theoretical value, thus all mobile protons are water protons. T_{2m} (T_g) of 90 wt % glucose cannot be obtained because all the water protons at T_g are immobile and thus no longer characterized by T_{2m}. T_{2m}(T_g) in maltose-water and glucose-water mixtures increases with increasing water content, even though T_g decreases. This means that the proton rotational mobility at T_g in these sugar-water glasses increases with increasing water content, opposite to the effect of water on the spin probe mobility.

In order to explain the fact that spin probe rotational mobility and water rotational mobility exhibit opposite behavior as a function of water content, additional structural information in malto-oligomer glasses is needed. Hereto two types of experiments have been performed.

	M_2 (10^9 s^{-2})
88 wt % glucose	8.6
79 wt % glucose	7.3
97 wt % maltose	8.3
85 wt % maltose	7.5

Table 2 Rigid limit values of the second moment M2 in glucose-, and maltose-D2O solutions.

Firstly, the effect of water content on the distance between the sugar molecules was estimated from the values of the second moment (M_2) (shown in Table 2). M_2 depends on anisotropic mobility and on the strength of the dipolar interactions between the protons[26]. At low temperatures where the mobility is too low to influence M_2, the rigid limit value of M_2 is solely determined by dipolar interactions (inversely proportional to the sixth power of the distance between the protons). This rigid limit value has two contributions. One is an intramolecular contribution, determined by the distance between the protons
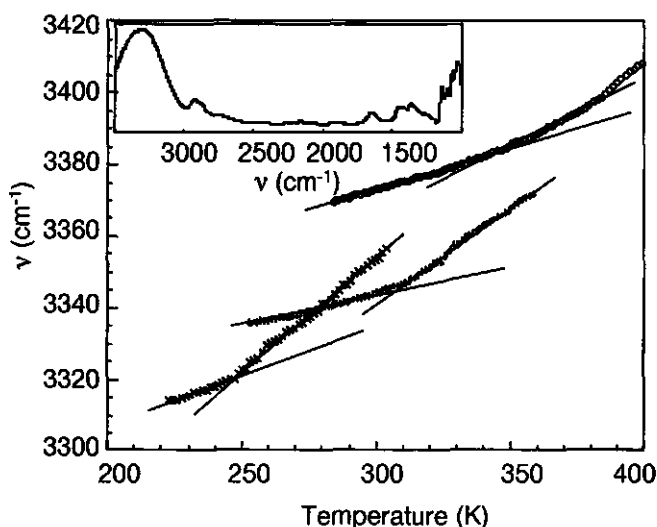
63

Figure 4 The wavenumber of the OH stretching vibration (v_{OH}) around T_g of maltose glasses equilibrated above 0% RH (o), 11 % RH (+) and 33% RH (x). The insert shows a FTIR spectrum of glassy maltose. Above 373 K evaporation of water is observed by an additional increase in v_{OH} with temperature.

within the molecules. The other is an intermolecular contribution dependent on the average distance between the molecules. In order to exclude the intra- and intermolecular contributions of the water, the water and hydroxyl protons of glucose and maltose were exchanged with deuterium, thus yielding the contribution due to the non-exchangeable sugar protons only. As a function of D_2O content, the intramolecular contribution will be constant in these samples. Thus, changes in the rigid limit value of M_2 in these samples will indicate changes in the average distance between the glucose rings. The results of the rigid limit values of M_2 in glucose and maltose-water glasses show that an increment in D_2O content leads to a reduction in M_2 . Thus, an increase in D_2O content yields an increase in average distance between the glucose rings.

Secondly, the packing of sugar and water molecules in glasses was studied by determining the strength of the OH bonds formed in these systems as obtained from FTIR. In Fig. 4 the wavenumber of the OH stretching bond (v_{OH}) versus temperature is shown for maltose-water samples. The glass transition

64

temperature is marked by an abrupt change in the temperature dependence of the hydrogen bond properties. This also follows from molecular dynamics simulations where the number and lifetime of hydrogen bonds increases at T_g [27-29]. The FTIR spectrum in the inset in Fig. 4 shows a broad featureless OH stretching bond around 3000 cm^{-1} which indicates that the sugar is in the glassy state, since a crystallized sugar shows several bands in this region[30]. The T_g values obtained from the FTIR experiments correspond to water contents between 1 and 20 wt % [8]. Addition of water increases the wavenumber of the OH stretching vibration at T_g.

Effect of molecular weight of the malto-oligomer

To compare the ESR results in freeze concentrated and concentrated glasses, the spin probe should reside in the freeze concentrated glass phase and not in the ice phase. We carried out two control experiments to check that the spin probe is not in the ice phase and that τ_R is not influenced by the amount of ice. The first experiment consisted of freeze concentrating a 20 wt % glucose solution to 80 wt % glucose. Thus the spin probe concentration should also increase fourfold. Since at high concentrations the spin probes exhibit spin-spin interactions which is reflected in the ESR spectra as line broadening, we compared the spin probe concentration at which line broadening first occurs at room temperature for a 80 wt % glucose glass with that for a freeze concentrated sample (data not shown). Indeed, 80% glucose glasses showed a four times higher spin probe concentration. Thus the spin probe, like glucose, is concentrated four times upon freezing, implying that the spin probe is not in the ice phase. The second experiment consisted of changing the initial amount of glucose between 20 and 55 wt %. All samples were freeze concentrated to approximately 80 wt % glucose. The amount of ice present in these samples will be decreased with increasing initial sugar content. We found that the rotational correlation time as a function of temperature was not influenced by

this variation in initial glucose concentration (provided that all samples were fully freeze concentrated by annealing at T_m' (data not shown)). Thus again the spin probe did not reside in the ice phase. We add that $\tau_R(T_g)$ in freeze concentrated malto-oligomer glasses and 80 wt % concentrated glasses is the same (Fig. 5).

The effect of the molecular weight of the malto-oligomer on the spin probe mobility at T_g is shown in Fig. 5. The value of T_g for a mixture of malto-oligomers increases upon increasing number average weigth of the mixture (Table 1). $\tau_R(T_g)$ decreases with increasing T_g implying that the spin probe mobility increases upon increasing molecular weight of the malto-oligomers. Also the water mobility increases with the size of the malto-oligomer as illustrated by the larger values of T_{2m} in maltose glasses compared to glucose glasses (Fig. 3). In order to compare the molecular packing within glucose and maltose samples, the rigid limit values of M_2 (Table 2) cannot be easily
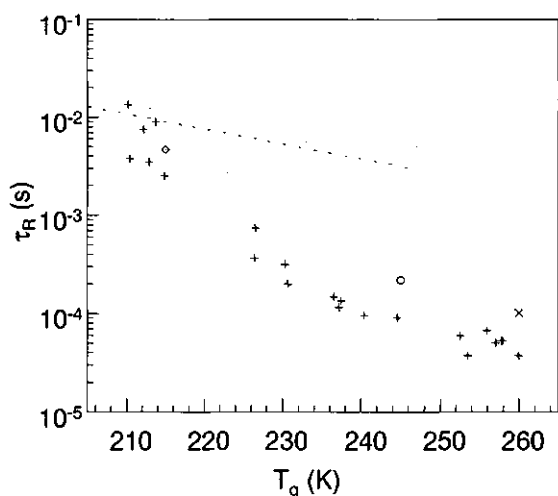

Figure 5 Rotational correlation times at the glass transition temperature τ_R (T_g) of TEMPOL in freeze concentrated mixtures of malto-oligomers (+) at the respective T_g compared with concentrated (about 80 wt %) glucose (◊), maltose (o), and maltoheptaose (x) glasses. The dotted line represents the glucose data of Fig. 2

compared, since both the intramolecular and the intermolecular contribution to M_2 changes with size of the molecules. The intramolecular contribution is different in glucose compared to maltose, since the covalent bond between the two rings in a maltose molecule, the average distance between the protons of the two rings in maltose is smaller than the average distance between the protons of two glucose rings.

Apart from an increase in $\tau_R(T_g)$, two other features of the spin probe mobility in concentrated glasses change with increasing size of the malto-oligomer (Fig. 1). One is that the apparent activation energy (E_{act}) for rotation of the spin probe below T_g is smaller in maltoheptaose than in glucose, while above T_g, E_{act} is larger in maltoheptaose than in glucose. The other is that E_{act} below T_g' decreases with molecular weight (Table 1). We add that the values for activation energy for rotational mobility of TEMPOL in sugar glasses are higher than reported previously[31-33], due to a recent improvement in the analysis of the ST-ESR spectra[24].

DISCUSSION

The first part of the discussion addresses the effects of *water content* on the water and spin probe rotational mobility in maltose and glucose glasses. In the second part, the effects of the *molecular weight* of the malto-oligomer on the water and spin probe mobility are discussed. We stress that the values for spin probe mobility change up to 7 orders of magnitude (Fig. 1) within the temperature range of $T_g \pm 50$ K. In order to compare the mobility in different glasses, T_g is taken as a reference point and we use the τ_R values of the spin probe as obtained at T_g. Consequently also ^{1}H-NMR and FTIR results are reported at T_g.

The value of τ_R of the spin probe at T_g is $\pm 10^{-2}$ s in glucose glasses[24]. We note that other ESR studies report values of $10^{-10} < \tau_R(T_g) < 10^{-8}$ s for spin probes in glasses of sugars [34], polymers [35, 36 37] and orthoterphenyl [38-40]. However τ_R values in that range do not characterize overall rotational motions but anisotropic motions such as librations of the spin probe molecule [41]. The value of $\tau_R(T_g)$ of the spin probe is small compared to $\tau_R(T_g)$ of glucose itself which is in the order of 100 s [42] . this indicates that spin probe mobility is decoupled from glucose mobility. This decoupling of probe mobility and matrix mobility has been reported to depend on the size of the probe molecule compared to the matrix molecules and on the interactions of the probe with its environment. The smaller the probe is compared to the matrix molecules, the more decoupling of its mobility[7, 43, 44].

Effect of water content

The mobility of the spin probe TEMPOL is measured as a function of temperature in glucose and maltose glasses with a water content between 10-30 wt %. From Fig. 2 it follows that spin probe rotational correlation time ($\tau_R(T_g)$) is reduced at increasing water contents. On the contrary the rotational mobility of the water at T_g is enhanced upon the addition of water (Fig. 3). Not only the rotational mobility of the water in maltose glasses is enhanced upon the addition of water, but also the sugar proton mobility at T_g increases with water content [19]. Thus, at T_g upon addition of water, both rotational mobility of the water and sugar protons in glucose-water and maltose-water glasses behave opposite to the $\tau_R(T_g)$ of the spin probe.

The fact that the behavior of spin probe mobility versus water content is opposite to the rotational water mobility as well as sugar proton mobility can be explained as follows. The spin probe mobility is determined by the interaction of the spin probe with its surroundings by means of the formation of OH bonds,

68

and by the molecular packing density. From analysis of the rigid limit values of M_2 it follows that the average distance between the carbohydrate molecules increases with increasing water content, explaining the increased water mobility at T_g, upon increasing water content. At the same time, the wavenumber of the OH stretching bond at T_g, $(v_{OH}(T_g))$(around 3300 cm^{-1}), is found to decrease upon increasing water content. This OH stretching bond is a broad band indicative for a variety of hydrogen bonds. Shifts in the wavenumber position of the peak indicate a change in the strength of the hydrogen bonds[20, 45]. In particular, a lower wave number of the OH stretching peak corresponds to a shorter average hydrogen bond length [45, 46]. Thus the observed decrease of $v_{OH}(T_g)$ upon increasing water content implies a denser hydrogen bonded network. This results in stronger hydrogen bonds between the spin probe and its environment and an increased molecular packing density. Both explain the observed decrease of $\tau_R(T_g)$ upon increasing water content.

Effect of the molecular weight of the malto-oligomer
Two types of glasses were studied. One type is the so-called concentrated (about 80 wt %) oligomer-water glass and the other is the so-called freeze concentrated glass (of mixtures of oligomers). The spin probe mobility at T_g was equal in both glass types The reasons that the freeze concentrated glasses are compared with 80 wt % malto-oligomer-water glasses are that the freeze concentration of small carbohydrates is reported to be around 80 wt % [1, 47, 48] and that the DSC values of T_g of 80 wt % glucose, maltose, and maltohexaose are close to their T_g' values[49, 50].

The spin probe mobility at T_g' is found to increase upon increasing molecular weight of the malto-oligomers (Fig. 5). This can be explained by a decrease in molecular packing density upon increasing molecular weight. Namely, the free volume at T_g is known to increase upon increasing molecular weight for small

polymers/oligomers[51] (monomers can be more densely packed than oligomers). Furthermore, the average radius of the molecular free volume at T_g is reported to increase with T_g [13, 52]. Thus, the spin probe experiences a lower molecular packing density in systems with larger oligomers.

In systems composed of mixtures of oligomers, T_g is found to be inversely proportional to the number average weight (M_n) (data in Table 1) and not to the weight average (M_w) as suggested before [53]. Different mixtures of malto-oligomers with the same M_n have the same T_g value and the same $\tau_R(T_g')$ (cf. Table 1). Thus M_n is the key parameter for $\tau_R(T_g')$. Using the above, M_n determines the molecular packing density and the volume available for rotational motion of the spin probe, and thus the mobility of the spin probe in mixtures of malto-oligomers.

Analogous to the increase of spin probe mobility at T_g with increasing molecular weight of the carbohydrate molecules, the water mobility is also increased upon increasing molecular weight. Also water translational diffusion increases with increasing molecular weight [54]. The jump distance for a water molecule is larger in samples with a higher molecular weight, which is ascribed to a less dense packing in systems containing longer oligomeric chains [54]. Also $\nu_{OH}(T_g)$ in FTIR experiments increases with the molecular weight of the oligomer [20]. Hence the hydrogen bond length increases [45, 46], indicative of a less dense hydrogen bonded network. This facilitates rotational mobility of the water as well of the spin probe at T_g. Thus the spin probe and water rotational mobility increase upon increasing molecular weight of the oligomers due to a decrease in molecular packing density.

Taking into account the above, the differences in the apparent activation energy (E_{act}) of spin probe mobility in malto-oligomer glasses above and below T_g can be explained. Namely, below T_g the apparent activation energy for

70

rotation decreases with increasing number average molecular weight (Table 1). This is because the spin probe is less hindered in its rotation in maltoheptaose compared to glucose, because of the lower packing density. In contrast, above T_g, the activation energy for rotation increases with molecular weight (Fig. 1). This can be explained as follows. Just above T_g the activation energy of rotation is a measure for the fragility [55, 56]. Polymer systems become more fragile with increasing molecular weight [56]. Also it is reported that the molecular free volume expands faster with temperature in the liquid state above T_g if the solution is more fragile[57]. Thus above T_g an increase in molecular weight implies a more fragile system and a higher molecular free volume, thus explaining the faster decreasing rotation in maltoheptaose compared to glucose, just above T_g.

Combining the results from the ESR, ^{1}H-NMR and FTIR measurements the following picture emerges. If water is added to a carbohydrate, the carbohydrate molecules are "pushed apart" and the "space in between is filled with water molecules". The water molecules rotate faster if the distance between the carbohydrate molecules is larger. At first instance, the overall packing at T_g of the water and carbohydrate molecules becomes denser at higher water content. Spin probe mobility at T_g decreases with increasing water content. The molecular packing also plays an important role if carbohydrate molecules of different molecular weight are compared. Oligomers are less dense packed than glucose, causing a higher water and spin probe mobility at T_g in oligomer containing systems.

We would point out a practical consequence the above. Low mobility of molecules encapsulated in glassy carbohydrates is needed for e.g. preservation and storage, and can be obtained if a strong interaction between the matrix and the encapsulated molecule is ensured. The size of the encapsulated molecules

should preferably be larger than the size of the matrix molecules. Taking into account the above, carbohydrate matrices are well suited to enclose polar molecules that have the ability to form strong hydrogen bonds with the matrix. Although the presence of water in a glass reduces the mobility of encapsulated molecules and would therefore be advantageous, we note that a lower temperature is needed to retain the mixture in a glassy state.

CONCLUSIONS

The apparent paradox that spin probe mobility decreases with increasing water content while water mobility at T_g increases in glucose and maltose glasses, is explained in terms of molecular packing. Upon increasing water content at T_g, the average distance between the carbohydrate molecules increases, leading to an increase in mobility of the water molecules. In parallel, the overall packing of the hydrogen-bonded network of water and carbohydrates molecules becomes denser at T_g , thus reducing spin probe mobility. The effect of molecular packing is also exemplified by comparing carbohydrate molecules of different molecular weight at constant water content, at T_g. Oligomers-water glasses are less densely packed than glucose-water glasses, therefore exhibiting a higher water and spin probe mobility compared to glucose-water glasses at T_g.

ACKNOWLEDGMENTS

REFERENCES

1. Y. Roos *Phase Transitions in Foods*; Academic Press: San Diego, 1995.

2. B. C. Hancock, S. L. Shamblin and G. Zografi. **1995**, *Pharm. Res*, 12(6), 799-806.

3. B. C. Hancock and G. Zografi. *J. Pharm. Sci.* **1997**, *86*, 1-12.

4. J. Buitink, M. M. A. E. Claessens, M. A. Hemminga and F. A. Hoekstra. *Plant Physiol.* **1998**, *118*, 531-541.

5. B. J. Aldous, F. Franks and A. L. Greer. *J. Mat. Sc.* **1997**, *32*, 301-308.

6. C. A. Oksanen and G. Zografi. *Pharm. Res.* **1993**, *10*, 791-9.

7. D. Champion, H. Hervet, G. Blond, M. Le Meste and D. Simatos. *J. Phys. Chem. B* **1997**, *101*, 10674-9.

8. T. R. Noel, R. Parker and S. G. Ring. *Carbohydr. Res.* **1996**, *282*, 193-206.

9. R. J. Elwell and R. A. Pethrick. *Eur. Polym. J.* **1990**, *26*, 853-856.

10. S. L. Anderson, E. A. Grulke, P. T. Delassus, P. B. Smith, C. W. Kocher and B. G. Landes. *Macromolecules* **1995**, *28*, 2944-2954.

11. R. M. Hodge, G. P. Simon, M. R. Whittaker, D. J. T. Hill and A. K. Whittaker. *J. Polym. Sci. B* **1998**, *36*, 463-471.

12. R. M. Hodge, T. J. Bastow, G. H. Edward, G. P. Simon and A. J. Hill. *Macromolecules* **1996**, *29*, 8137-8143.

13. H. L. Li, Y. Ujihira, A. Nanasawa and Y. C. Jean. *Polymer* **1999**, *40*, 349-355.

14. K. Suvegh, A. Domjan, G. Vanko, B. Ivan and A. Vertes. *Macromolecules* **1998**, *31*, 7770.

15. M. Forsyth, P. Meakin, D. R. MacFarlane and A. J. Hill. *Electrochim. Acta* **1995**, *40*, 2349.

16. A. J. Hill, D. R. MacFarlane, J. Li, P. L. Jones and M. Forsyth. *Electrochim. Acta* **1998**, *43*, 1481-1484.

17. R. C. Macqueen and R. D. Granata. *J. Polym. Sci. B.* **1993**, *31*, 971-982.

18. J. Borek and W. Osoba. *J. Polym. Sci. B* **1998**, *36*, 1839-1845.

19. I. J. van den Dries, D. van Dusschoten and M. A. Hemminga. *J. Phys. Chem.* **1998**, *102*, 10483-10489.

20. W. F. Wolkers, H. Oldenhof, M. Alberda and F. A. Hoekstra. *Biochim. Biophys. Acta* **1998**, *1379*, 83-96.

21. M. A. Hemminga. *Chem. Phys. Lipids* **1983**, *32*, 323-383.

22. M. A. Hemminga, P. A. de Jager, D. Marsh and P. Fajer. *J. Magn. Reson.* **1984**, *59*, 160.

23. D. D. Thomas, L. R. Dalton and J. S. Hyde. *J. Chem. Phys.* **1976**, *65*, 3006-3024.

24. I. J. van den Dries, P. A. de Jager and M. A. Hemminga. *J. Magn. Res.* **1998**, *131*, 241.

25. A. Abragam *The principles of nuclear magnetism*; Clarendon Press: Oxford, 1961.

26. V. J. McBrierty and K. J. Packer *Nuclear magnetic resonance in solid polymers*; Cam. Univ. Press: Cambridge, 1995.

27. E. R. Caffarena and J. R. Grigera. *in press* **1999**.

28. E. R. Caffarena and J. R. Grigera. *Carbohydrate Research* **1997**, *300*, 51-57.

29. E. Caffarena and J. R. Grigera. *J. Chem. Soc. Faraday Trans.* **1996**, *92*, 2285-2289.

30. E. T. G. Lutz and J. H. van der Maas. *J. Mol. Struct.* **1994**, *324*, 123-132.

31. M. J. G. W. Roozen, M. A. Hemminga and P. Walstra. *Carbohydr. Res.* **1991**, *215*, 229-237.

32. M. J. G. W. Roozen and M. A. Hemminga. *Spec. Publ. - R. Soc. Chem.* **1991**, *82*, 531-536.

33. M. J. G. W. Roozen, P. Walstra, T. van Vliet and M. A. Hemminga. A spin probe ESR study of sugar water mixtures in the liquid and glassy state. In *Electron spin resonance applications in organic and bioorganic materials*; B. Catoire, Ed.; Springer Verlag: Berlin, 1992; Vol. Appl. Org. Bioorg. Mater., Proc. Eur. Meet., 1st (1992), Meeting Date 1990; pp 31-51.

34. S. A. Dzuba, Y. A. Golovina and Y. D. Tsvetkov. *Appl. Magn. Reson.* **1993**, *5*, 31-37.

35. J. I. Spielberg and E. Gelerinter. *J. Chem. Phys.* **1982**, *77*, 2159-2165.

36. A. L. Kovarski, J. Placek and F. Szocs. *Polymer* **1978**, *19*, 1137-1141.

37. K. Hamada, T. Iijima and R. McGregor. *J. Polym. Sci., Part B: Polym. Phys* **1987**, *25*, 1299-1310.

38. L. Andreozzi, F. Cianflone, C. Donati and D. Leporini. *J. Phys. Condens. Matter* **1996**, *8*, 3795-3809.

39. L. Andreozzi, A. Dischino, M. Giordano and D. Leporini. *J. Phys. Condens. Matter* **1996**, *8*, 9605-9608.

40. L. Andreozzi, A. Dischino, M. Giordano and D. Leporini. *Europhys. Lett.* **1997**, *38*, 669-674.

41. S. A. Dzuba. *Physics Letters A* **1996**, *213*, 77-84.

42. D. van Dusschoten, U. Tracht, A. Heuer and H. W. Spiess. *in preparation* .

43. M. T. Cicerone, F. R. Blackburn and M. D. Ediger. *J. Chem. Phys.* **1995**, *102*, 471-479.

44. G. Heuberger and H. Sillescu. *J. Phys. Chem.* **1996**, *100*, 15255-15260.

45. G. A. Jeffrey *An introduction to hydrogen bonding*; Oford University Press: Oxford, 1997.

46. A. Novak. Hydrogen bonding in solids. Correlation of spectroscopic and crystallographic data. In *Structure & bonding*; Deutz, Ed.; Springer Verlag: Zurich, 1974; Vol. 18.

47. S. Ablett, A. H. Darke, M. J. Izzard and P. J. Lillford *Studies of the glass transition in malto-oligomers*; Nottingham University Press: Nottingham, 1993.

48. S. Ablett, M. J. Izzard and P. J. Lillford. *J. Chem. Soc. Far. Trans.* **1992**, *88*, 789-794.

49. P. D. Orford, R. Parker, S. G. Ring and A. C. Smith. *Int. J. Biol. Macromol.* **1989**, *11*, 91-96.

50. R. Parker and S. G. Ring. *Carbohydr. Res.* **1995**, *273*, 147-55.

51. T. G. Fox and S. Loshaek. *J. Polym. Sci.* **1955**, *15*, 371.

52. J. Bartos. *Colloid Polym. Sci.* **1996**, *274*, 14-19.

53. L. Slade and H. Levine. *Food science and Nutrition* **1991**, *30*, 115.

54. R. H. Tromp, R. Parker and S. G. Ring. *Carbohydr. Res.* **1997**, *303*, 199-205.

55. R. Bohmer, K. L. Ngai, C. A. Angell and D. J. Plazek. *J. Phys. Chem.* **1993**, *99*, 4201.

56. E. Rossler, K. U. Hess and V. N. Novikov. *J. Non-Cryst. Sol.* **1998**, *223*, 207-222.

57. J. Bartos and J. Kristiak. *J. Non-Cryst. Sol.* **1998**, *235*, 293-295.

5

A relation between a transition in molecular mobility and collapse phenomena

in glucose–water systems

Ivon van den Dries, Klaas Besseling, Dagmar van Dusschoten, Marcus Hemminga, and Erik van der Linden

ABSTRACT

Surprisingly, in concentrated glucose glasses with water contents between 10 and 30 wt%, two transitions in mobility of the sugar protons are observed using proton magnetic resonance techniques. The first transition in mobility is positioned at the glass transition temperature while the second is about 20 to 30 degrees higher. The temperature of this second transition is found to depend on water content, resulting in a new line in the state diagram of glucose-water mixtures. In freezeconcentrated glucose glasses we find two similar transitions. We interpret the second transition as the socalled crossover temperature, where the dynamics changes from solidlike to liquidlike. In freezeconcentrated glasses an increase in the amount of ice melting per degree is observed just above the temperature of the second transition. We propose that both in concentrated and freezeconcentrated glucose glasses, this second transition relates to so-called collapse phenomena in glasses.

INTRODUCTION

Sugars in foods exist as crystals, in an amorphous state or in solution. The amorphous state of sugars can be formed during cooling from a melt or by rapid removal of the solute from the sugar solution by means of dehydration or the formation of ice. In these processes oversaturated sugar solutions are produced and if the sugar does not crystallize, an amorphous sugar matrix or so-called sugar glass is formed[1]. Bringing the temperature of the sugar glass above its so-called glass transition temperature, the sugar matrix shows macroscopically visible changes in physical properties compared to below the glass transition temperature (T_g). These changes are generally attributed to a reduction in viscosity upon increasing temperature above the glass transition temperature, such that flow on a practical timescale occurs. It is found that the timespan that is required for the visible change in physical properties to occur depends on the temperature. In fact, this timespan decreases with increasing temperature, above T_g. It is also found that this timespan exhibits an abrupt decrease at a specific temperature. This temperature is usually referred to as the collapse temperature [2, 3]. For sugar glasses, collapse temperatures and the concomitant collapse phenomena occur in general 15-25 degrees above T_g[1].

Examples of collapse phenomena include (1) the stickiness and caking of powders; (2) plating of particles on amorphous granules; and (3) structural collapse of freeze dried materials[4].

The onset of collapse phenomena is still under debate. For example, collapse phenomena in glasses that are formed due to removal of water from the sugar solution by means of ice formation (i.e. freezeconcentrated glasses) have been related to the so-called onset of ice melting transition which can be observed using Differential Scanning Calorimetry (DSC)[5, 6]. This transition is observed in a DSC curve as a shoulder on the ice-melting peak. It was suggested[6] that

collapse phenomena in other types of glasses, such as glasses obtained by drying, have the same origin as this onset in ice melting transition in freeze-concentrated systems.

In view of our interest in the onset of the above described collapse phenomena we studied two types of glucose glasses from a molecular mobility point of view. One type of glass is the so-called freeze-concentrated glass, and the other type is obtained by cooling from the melt (i.e. concentrated glass). Specifically we determined the molecular mobility of sugar and water using a proton Nuclear Magnetic Resonance (^{1}H-NMR) technique [7, 8]. In the freeze concentrated glucose glasses we also used this technique to determine the glucose concentration in the solution phase during ice melting. In both types of glasses we observe a transition in molecular mobility at a temperature situated above the glass transition temperature and we propose that this transition in molecular mobility is related to the origin of collapse in both types of glucose glasses.

MATERIALS AND METHODS

Preparation of samples

Sugar glasses were prepared in two ways. 1) *Concentrated* glucose-water glasses where prepared by mixing the appropriate amounts of sugar and water, melting the mixture, and quickly cooling it below the glass transition temperature. Concentrated glasses prepared this way were compared with concentrated glasses prepared by freezedrying and because no differences were found we only used glasses prepared from the melt. 2) *Freezeconcentrated* glucose glasses were prepared by freezeconcentrating a sugar solution along the following route. Upon cooling 20 wt % solutions of sugars, ice is formed. Due to this freezing out of water, the sugar concentration

in the solution phase increases up to approximately 80 wt %. Upon further cooling a 80 wt % sugar glass is formed. The resulting material is heterogeneous as it contains small ice crystals dispersed in a sugar glass. Anhydrous glucose was obtained from Jansen Chimica, glucose monohydrate from Merck. Glucose with deuterated hydroxyl groups was prepared by dissolving the monohydrate (1 g) in D_2O (5 ml) and subsequently freeze-drying before adjusting the water content with D_2O. For the NMR samples appropriate amounts of sugar and water were mixed in 5 mm NMR tubes and sealed to prevent water evaporation.

^{1}H-NMR spectroscopy

^{1}H NMR measurements were performed on a Bruker AMX 300 spectrometer equipped with a Bruker 5 mm proton probe operating at a resonance frequency of 300.13 MHz. The temperature was regulated with a nitrogen temperature controller. In this way, the temperature stability was within ±0.5 K. A spectral width of 500 kHz was used. The duration of the 90° pulse was 4.5 µs. The free induction decays (FID) are averages of 4 - 256 scans having 2048 data points. Using a repetition time of 10 s, the signal of ice is saturated. We estimate that the signal of ice contributes less than 15% to total amplitude of the FID by comparing the signal of ice (without sugar) with the signal of the freezeconcentrated glasses.

The NMR spectrum of the immobile proton fraction is assumed to be a rectangular line shape with a total width 2b, convoluted with a Gaussian line shape with a standard deviation given by parameter a [9, 10]. Superimposed on this rectangular lineshape is a Lorentzian lineshape arising from the mobile protons. For the analysis of the NMR, the FIDs F(t) were fitted by the following equation[8]:

$$F(t) = A \exp\left[\frac{-a^2 t^2}{2}\right] \frac{\sin bt}{bt} + B \exp\left[\frac{-t}{T_{2m}}\right] \tag{1}$$

where A and B denote the amplitudes originating from immobile and mobile protons, respectively, and T_{2m} is the spin-spin relaxation time of the mobile proton fraction. The lower limiting value of T_{2m} is $2*10^{-5}$ s, which is about $2b$[8], and corresponds to an upper limit of the rotation correlation time τ_R of $3*10-6$ s calculated using the Bloembergen-Purcell-Pound theory[9]. T_{2m} is proportional to τ_R if $1/\tau_R <<$ than the Larmor frequency[9]. Protons with τ_R values of $3*10-6$ s will be called immobile. Upon decreasing temperatures, the values of T_{2m} and B decrease. However, if the T_{2m} value obtained by fitting to Eq. 1 becomes smaller than $2*10^{-5}$ s, which indicates that there is no longer a mobile proton fraction, the data are fitted to the first part of Eq. 1 only. The NMR signal arising from the ring and exocyclic protons in deuterated glucose samples is also fitted to the first part of Eq. 1. On increasing the temperature, the dipolar interactions start to average out and the broad component sharpens up. As long as the FID's show oscillations, characteristic for the rectangular line shape of the immobile proton fraction, they are well fitted with Eq 1. Finally, the oscillatory character of the FID is lost and then the FID's are fitted to a biexponential function.

The second moment (M_2) is calculated using $M_2 = a^2 + 1/3b^2$ where a and b are determined from fitting the FID with Eq. 1 [9]. M_2 of the immobile protons is a measure of incompletely averaged dipolar interactions [8, 10]. In the analysis of M_2 of the immobile protons, the following points should be taken into account[8]. A reduction of M_2 takes place if 1) the proton density is lowered (since the dipolar interactions decrease with the sixth power of the proton-proton distance), and/or if 2) anisotropic motions or very slow isotropic rotations increase, since both partly average out the dipolar interactions.

DSC

Samples with a weight between 10 and 20 mg were measured using a Pyris 1 DSC (Perkin-Elmer) at a cooling and heating rate of 80 and 10 K/min, respectively. The samples are always cooled to 190 K before reheating, until the temperature of annealing. After annealing, all samples are cooled to 190 K, which is the starting temperature for the heating scan, except for the ones annealed at 180K. From the heating scans the onset of the glass transition T_g' and of the onset of ice melting (T_m') are determined.

RESULTS

Concentrated glucose-water mixtures

Upon warming concentrated glucose glasses with water contents between 10 and 30 wt %, two transitions are observed in the slope of the second moment (M_2) of the immobile protons against temperature (Fig. 1A). The first transition occurs at the glass transition temperature (T_g) (see Fig. 2) and the second transition is observed at T= T_{tr2} where T_{tr2} is 20-30 degrees higher than T_g. Note that in solutions with a glucose content of 70 and 73 wt %, T_g is too low to be measured and only T_{tr2} is observed. The second transition is also apparent as an increase in the slope of the spin-spin relaxation time (T_{2m}) against temperature (Fig. 1B). Note that the glass transition will not appear in Fig. 1B since there are too few mobile protons at T_g. The temperatures of the second transition as a function of water content define the line BAC in the state diagram (Fig. 2).

In order to exclude the possibility that the second transition in M_2 may be due to the fact that the fraction of immobile protons decreases we used partly deuterated glucose samples (such that all exchangeable protons are deuterated), ensuring that all protons would remain immobile in the temperature
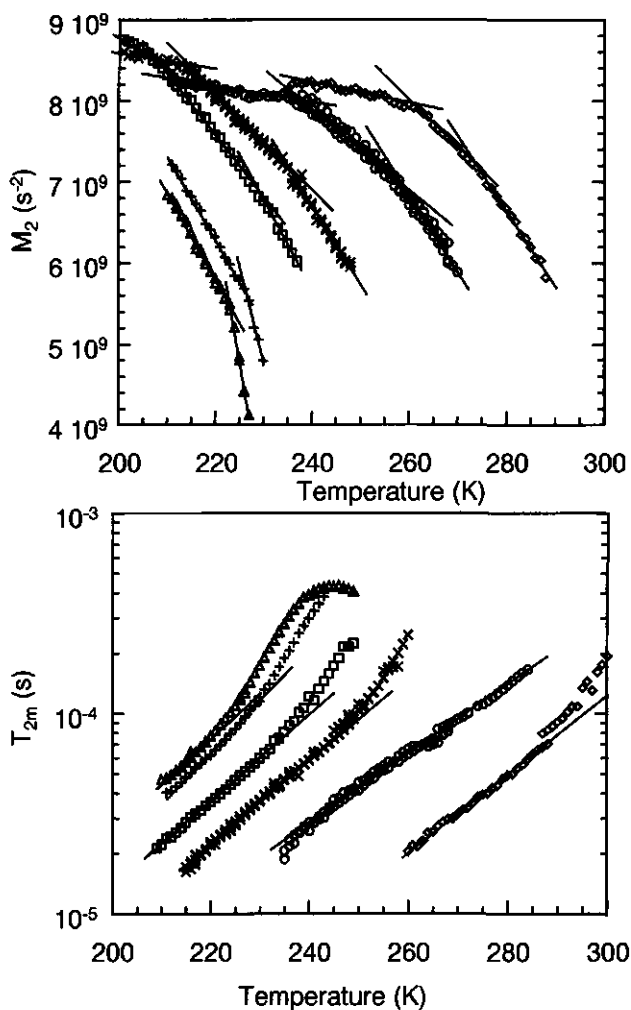
Figure 1 The second moment (M_2) of the immobile protons (Fig. 1A) and the spin-spin relaxation time (T_{2m}) of the mobile protons (Fig. 1B) versus temperature for 70 ($\triangle$), 73 (+), 75 ($\square$), 80 (x), 85 (o), and 90 wt % ($\lozenge$) glucose solutions.

range studied. The same two transitions were observed (data not shown), leading to the conclusion that the second transition is related to changes in mobility of the immobile protons.
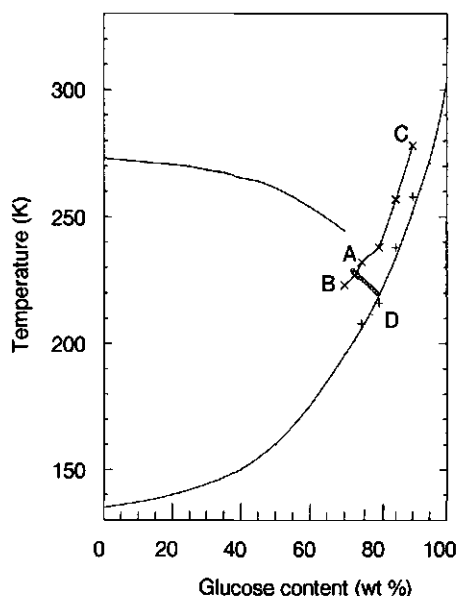
Figure 2 State diagram of glucose. The freezing point depression data are taken from Luyet[25] and Young[26]. The glass transition data are taken from Noel et al.[12]. Line BAC represents the T_{tr2} temperature. Point D is T_g' of glucose.

Freezeconcentrated glucose-water mixtures

In freezeconcentrated glucose glasses we also observed two transitions in M_2 as a function of the temperature, similar to the ones as observed in concentrated glasses. The interpretation of these transitions in freeze concentrated is however more tedious than it is for concentrated glasses. Namely, the transitions in freezeconcentrated glasses could also be related to changes in the ice melting process, such as the rate of ice melting or the amount of ice that melts.

In order to exclude these possibilities we first studied the influence of the ice melting process on the molecular mobility. In order to avoid effects of delayed ice formation in the temperature range of interest. We first identified the conditions to obtain freeze concentrated glasses that are maximally concentrated. Subsequently, these maximally freezeconcentrated glasses were
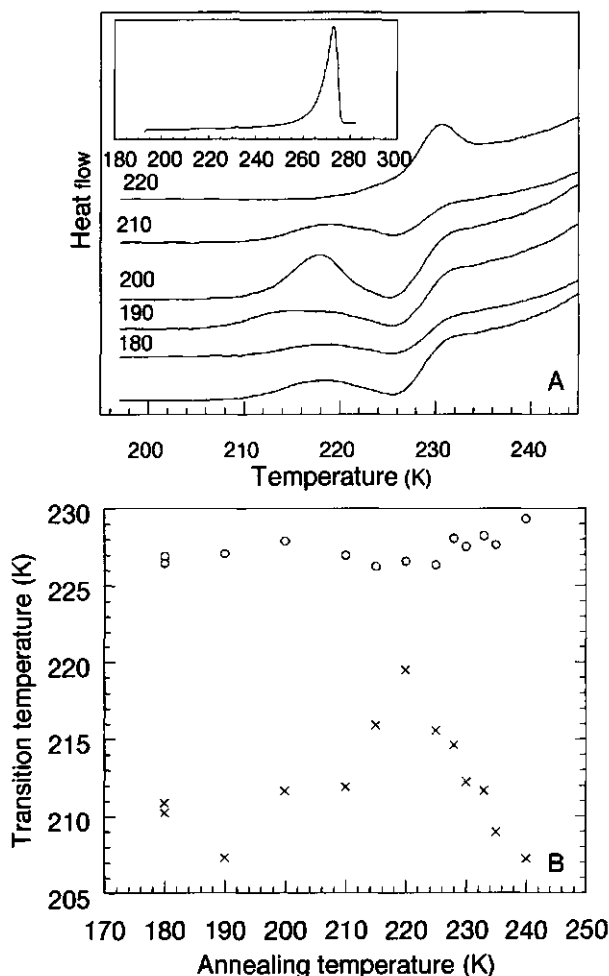
Figure 3 The inset of Fig. 3A shows a DSC scan of 20 wt% glucose. For the samples annealed at temperatures indicated at each scan the temperature range from 195 to 245 is enlarged, to show the effect of annealing on the transition temperatures. The scan without temperature is not annealed. In Fig. 3B the onset temperatures of the glass transition (T_g) (x) and the second transition (T_{tr2}) (o) are shown as a function of annealing temperature.

used to study the icemelting process. Finally, all these findings allow us to draw conclusions about the nature of the second transition.

First the *conditions to obtain freezeconcentrated* glasses were investigated as follows. The process of freeze concentration was studied using DSC, following the annealing protocols of Ablett[11]. In the inset of Fig. 3A DSC

heating traces of a freeze concentrated glucose glass are shown as a function of temperature. The temperature range between 195 K and 245 K is enlarged to show temperature shifts of the glass transition temperature as a function of the annealing temperature (Fig. 3A). In the DSC heating traces of freeze concentrated glucose between 195 and 245 K two thermal transitions are observed, first the glass transition temperature, denoted by T_g', and secondly a second transition temperature T_m', where the prime refers to the fact that the glass is freeze concentrated. The onset temperatures of these transitions are shown in Fig. 3B as a function of the annealing temperature.

A quench cooled glucose glass has a T_g value of 210 K and annealing above 210 K leads to ice formation. Formation of ice increases the glucose concentration and thus increases the glass transition temperature (Fig. 3B). The maximum glass transition temperature occurs at 220 K. Taking into account that a T_g' value of 220 K corresponds to the T_g value of a concentrated 81 wt % glucose-water glass [12], we deduce that the maximum freeze concentration should be 81 wt %. We note that Fig. 3B also shows annealing temperatures below 210 K. If the glass is annealed below 210 K, overshoot peaks are observed at the glass transition temperature. This is for example clearly visible for an annealing temperature at 200 K (cf. Fig. 3A). This overshoot slightly decreases the T_g' onset value. Therefore the decreases in T_g' at annealing temperatures below 210 K are artifacts, due to aging of the glass.

We note that the process of freeze concentration during annealing as studied by DSC could in principle also be followed by ^{1}H-NMR (since the water mobility is decreased during this process, implying a decrease in the spin-spin relaxation time, T_{2m}. However, the maximum cooling rate in a NMR experiment is relatively low, which causes the process of freeze concentration to be always completed during cooling. Therefore the resulting T_{2m} values as a function of annealing temperature remain constant (data not shown).

Using the findings above we concluded for our NMR experiments that annealing for one hour at 220 K yielded maximally freeze concentrated glucose glasses. These freeze concentrated glucose glasses were subsequently used to study the influence of the ice melting process on the second transition.

The *influence of the icemelting process* on the molecular mobility in freeze concentrated glucose glasses was studied by means of determining M_2, T_{2m}, and the amount of mobile protons (B) as a function of temperature. The results are shown in Fig. 4A, 4B and 4C, respectively. The signal of the ice itself is not observed because it was saturated before each experiment. Immediately above the glass transition (220 K), ice starts to melt. This is observed as an increase in the amount of the mobile protons, which is due to an increase of the amount of water (Fig. 4C). Around 235 K an increase in the amount of ice melting per degree is observed as an increase in the derivative of B towards temperature (Fig. 4C). This increase in the amount of ice melted per degree will from now on referred to as an increase in the ice-melting rate.

The mobility of the glucose protons shows two transitions exhibited by abrupt changes in the temperature dependence of M_2 (Fig. 4A). The first transition corresponds to the glass transition around 220 K as was observed with DSC for freezeconcentrated glucose glasses (Fig. 3B). The temperature of the first transition is slightly influenced by the heating rate of the experiment (as expected for a glass transition). At 230 K, a second transition in the mobility of the solid protons is observed (Fig. 4A). Note that at temperatures above the second transition the solid protons become so mobile that they belong to the mobile fraction and no longer are characterized by M_2. Therefore only one data point of M_2 is reported above 230 K.

T_{2m} above 220 K (= T_g') shows a stronger increase with temperature in a freeze concentrated glass than in a 80 wt % glucose solution (Fig. 4B). This implies that the mobility of the water protons increases (due to ice melting). Namely, T_{2m} around T_g' is indicative for water rotational mobility because at T_g' all mobile protons are water protons. This follows from the fact that around T_g' the ratio of amplitudes of the mobile (B) and immobile (A) component in the FID (B/A) is smaller than the theoretical B/A value in the case of all water protons being mobile and all sugar protons being immobile in a 80 wt % system[8]. Around 230 K, where the solid protons undergo a second transition (Fig. 4A), the mobility of the mobile protons also increases, which follows from the increase in slope of T_{2m} against temperature (Fig. 4B). T_{2m} no longer increases around 240 K probably because the ring protons of glucose start to contribute to the mobile proton signal.

To interpret the above described transitions in M_2 and T_{2m} in freeze concentrated glasses similar to the transitions in concentrated glasses, we should exclude the possibility that an abrupt increase in ice melting rate would cause the second transition. Inspired by the idea of Franks that ice dissolution would be kinetically hindered just above T_g [6] and therefore would be dependent on the heating rate, we studied the water mobility and magnitude of the mobile fraction as a function of heating rate (Fig. 4B & 4C). The highest heating rate in the NMR experiments is 0.6 K/min, which is one order of magnitude smaller than in the DSC experiments where the heating rate equals 10 K/min. The lowest heating rate is 0.023 K/min (i.e. 1 K per hour). This time scale of 1 K/hour lies in the same range as that of ice formation and ice melting during annealing, as observed with DSC.
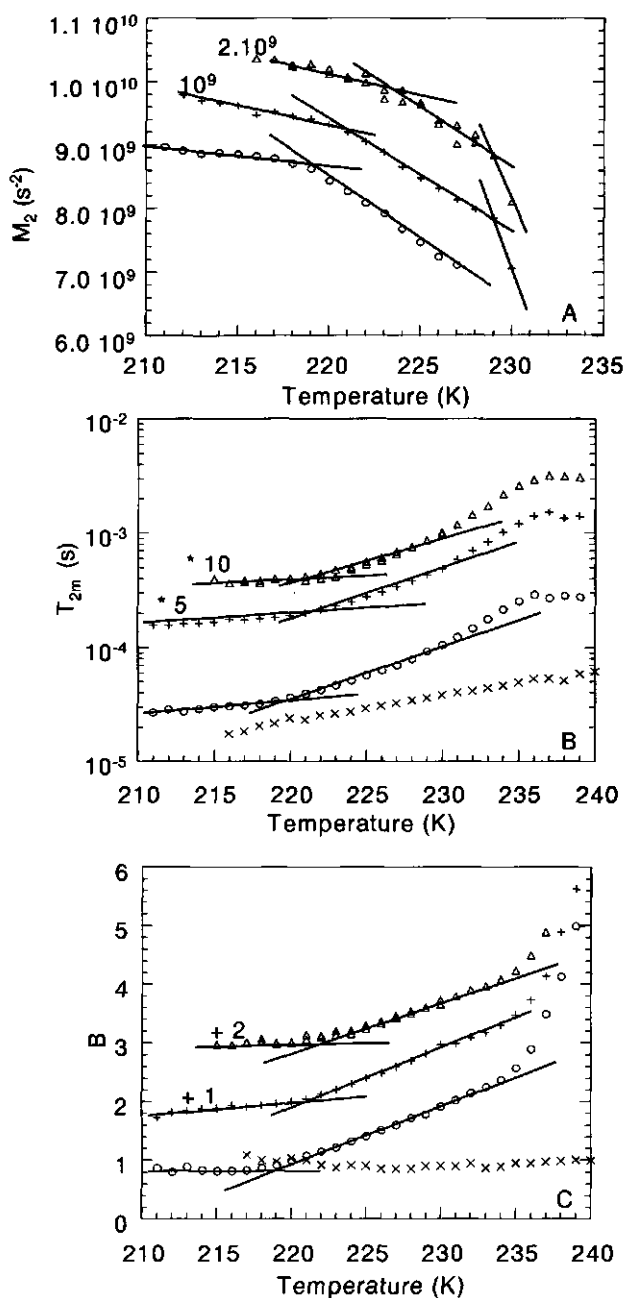
Figure 4 The second moment (M₂) of the immobile protons (Fig. 4A), the spin-spin relaxation time (T₂m) of the mobile protons (Fig. 4B), and the amplitude (B) of the mobile protons (Fig. 4C) versus temperature for maximally freezeconcentrated glucose solutions heated with a rate of 100 (◊), 380 (+), and 3600 (o) seconds per degree and for a 80 wt % glucose glass (x) heated with a rate of 100 s per degree. The amplitudes (B) are divided by the amplitude at 220 K to scale the results. The results in Fig. 4A, 4B and 4C are shifted for clarity.

We would like to point out two observations. 1) Both transitions, T_g' and T_{tr2}', are observed separately for various heating rates (Fig. 4A & 4B). 2) From figure 4 C it follows that the slope of B versus T, indicative of increase of the mobile fraction, and thus of rate of ice melting, is independent of heating rate, between 220 K and 235 K. Note that there is a slight decrease in T_g' with decreasing heating rate (as expected). These two observations lead us to conclusion that the second transition is not caused by a change in ice melting rate.

The state diagram of glucose around the intersection point of the freezing point depression line and the glass transition temperature line (Fig. 2) was constructed as follows. The concentration of glucose at temperatures between 220 and 230K is calculated from the amount of ice melted (this in turn can be calculated from the increase in amplitude B (Fig. 4C)). For example, at 220 K where the sample is a 81 wt % glass, it is known what the value of B/A should be if all water protons are mobile and all sugar protons are immobile. This ratio is 0.39. The measured value of B/A however is 0.2 (data not shown). The percentage of mobile water protons turns out to be 60%. Taking a starting sample consisting of 20 g glucose and 80 g of water, the resulting freeze concentrated sample will consist of 20 g glucose, 5.2 g water and 74.8 g ice (using a glucose concentration of 81 wt %). The amplitude B at 220 K will be caused by 0.6 * 5.2 g = 3.1 g water. At 230 K the signal B is 1.9 times larger. Thus 2.8 g ice has melted during heating from 220 K to 230 K. The solution concentration is calculated to be 72 wt %.

This value for the glucose concentration can also be determined from values for T_{2m} by comparing the values of T_{2m} in freeze concentrated glucose at 230 K with the T_{2m} values in concentrated glucose solutions at 230 K (Fig. 1B). This yields a concentration of glucose of 73 wt %. Thus, the values of the glucose concentration at 220 K and 230 K are 81 and 73 wt % , denoted by A and D in

88

the state diagram, respectively (Fig. 2). The low rate of ice melting between 220 and 230 K, which causes a linear increase in B, leads to the line AD in the state diagram (Fig. 2).

DISCUSSION

In this paper we have determined the molecular mobility in sugar-water systems in the temperature range around the glass transition temperature (T_g). Two types of glucose glasses have been investigated: 1) concentrated glucose glasses (prepared by mixing the appropriate amount of sugar and water, melting and subsequently cooling below T_g) and 2) Freezeconcentrated glucose glasses (prepared by cooling a 20 wt % glucose solution; due to ice formation during cooling, ultimately a 80 wt % glucose glass is formed). We will first discuss the results according to the division into these two types. Then we will discuss the similarity between the two types of glasses.

Concentrated glucose-water mixtures

By using ^{1}H-NMR, two transitions in the mobility of the glucose protons in glucose glasses with a water content between 10 to 30 wt % have been observed. We propose that the second transition temperature may be identified as the so-called crossover temperature, where the dynamics of the system changes from liquid like to solid like upon cooling. We will now discuss the various changes in dynamics of a glass system in more detail and relate these changes to changes in M_2, thus clarifying our proposition. Above the crossover temperature the dynamics is dominated by diffusional motion leading to a single relaxation process: α-relaxation [13]. Below the crossover temperature an additional relaxation process shows up, the so-called Johari-Goldstein β-relaxation, which has a different temperature behavior [13] and can be visualized

as "rattling of a molecule inside a cage formed by its neighbors". In the temperature region between T_g and the crossover temperature these cages still undergo collective distortions, leading to diffusion (α-relaxation). At temperatures below T_g only the motion of a molecule inside a cage persists [14].

Using this picture it follows that below T_g the mobility, denoted by the parameter M_2 should only be influenced by small angular anisotropic motion of the protons (i.e. β relaxation processes). Since the angle and rate of these anisotropic motions increases slightly with temperature below T_g [15], the dipolar interactions will be averaged out more which results to a decrease of M_2 with increasing temperature below T_g. Above T_g, both diffusional motion (α-relaxation) and small angular anisotropic motion (β-relaxation) will average out the dipolar interactions. This results in a stronger decrease of M_2 with temperature above compared to below T_g. Therefore the glass transition is observed as the first change in the temperature dependence of M_2. At this glass transition temperature all protons still belong to the immobile fraction. Upon heating above T_g, the α and β relaxation processes will have to merge at some temperature, which defines a second transition temperature (defined as the crossover temperature). Thus a second transition is expected. This is indeed observed as the second change in the temperature dependence of M_2 (at T_{tr2}). Thus this second transition is likely to signify the cross over temperature.

We add that we observed that at T_{tr2} the first sugar protons become mobile, corresponding to a $\tau_R > 3*10^{-6}$ s. This may also indicate that the second transition signifies the crossover temperature. Namely, in general, the timescale associated with crossover temperatures lies between 10^{-8} s and 10^{-6} s [13, 16, 17]. Our τ_R value is in the same range as observed at the crossover temperature in other glass formers such as sorbitol [18, 19], polybutadiene [16], orthoterphenyl [16].

We note that in a deuterium NMR study of 75 wt % glucose solutions a bifurcation of the α and β relaxation is shown around 240 K [20]. This is at a slightly higher temperature than the T_{tr2} transition we observe at 230 K (Fig 1A). The discrepancy may be due to uncertainties in the glucose concentration due to the presence of a small amount of ice [20].

Taking into account the above-described view on transitions in the dynamics of glass systems we may also relate the abrupt increase in mobility of the sugar at T_{tr2} to so-called collapse phenomena as follows. In general, collapse is attributed to a decrease in viscosity above T_g until a value of 10^8 Pa s. where flow on practical timescales is observed. This phenomenon is usually observed as something that occurs suddenly. We suggest that an underlying transition in molecular mobility causes this sudden change in flow and that this transition occurs at $T=T_{tr2}$. We note that it was already shown for a number of glass formers that the temperature dependence of the viscosity changes at the crossover temperature [21]. Furthermore, in bending experiments, also two transitions were observed for the loss and storage moduli as a function of temperature[22, 23], one at T_g (where the storage modulus decreases slightly above T_g) and a second transition 15 degrees above T_g (showing a stronger decrease in the storage modulus) This second transition was also related to collapse [22].

In short, we observe a transition in molecular mobility in concentrated glucose-water mixtures above T_g and interpret this transition as a crossover temperature, where the dynamics changes from solid like to liquid like. The temperature of T_{tr2} depends on water content, resulting in an extra line B-A-C in the state diagram (Fig. 2). We suggest that the second transition in molecular

mobility, above T_g, is the underlying cause of collapse phenomena in concentrated glucose-water glasses.

Freezeconcentrated glucose-water mixtures

Two transitions in molecular mobility are observed as changes in the derivatives of M_2 and T_{2m} with temperature (Fig. 4A and 4B). Also the amount of mobile protons as a function of temperature shows two transitions (Fig. 4C). The first transition occurs at the glass transition temperature and the second transition at 230 K. Both transitions are not affected by heating rate. Furthermore, the increase in the amount of mobile protons, indicative of the amount of ice melting per degree, is not affected by the heating rate (slope of B versus T in figure 4 C). This leads us to the conclusion that the second transition is not caused by a change in ice melting rate. The second transition is also not related to the onset of ice melting, since the amount of water in our experiments was found to increase immediately at the glass transition temperature, and not at a higher temperature.

We note that using DSC measurements, also two transitions can be observed. One at T_g' (=220 K) and the other at 227 K (Fig. 3 B). It was suggested that the second transition is due the fact that ice melting would be kinetically hindered above T_g' [6, 11, 24]. This in turn was proposed to be related to the fact that mixing of the melt water with the glucose solution that is surrounding the ice crystals would be hindered by the high viscosity of the glucose solution. The second transition would then signify the transition from kinetically hindered to normal equilibrium ice melting [6]. This reasoning would imply that at extremely low heating rates, where the diffusion of the melted ice into the sugar matrix would not be hindered, this second transition would have to coincide with T_g' [6, 11, 24]. Our molecular mobility data suggest a different

92

explanation for the occurrence of two transitions since they show that at lower heating rates both transition temperatures do not coincide. Hence, the second transition is not coupled to the onset of ice melting nor to the rate of ice melting within the temperature range between 220 K and 230 K.

Similarities between freeze concentrated and concentrated sugar glasses

We propose that, analogous to concentrated sugar-water mixtures, the second transition in M_2 signifies the crossover temperature of the concentrated glucose-water mixture surrounding the ice where the dynamics of the glucose-water mixture changes from solid like to liquid like.

Although in concentrated glucose glasses the second transition occurs 20-30 degrees above T_g while in freeze concentrated solutions a temperature difference of only 10 degrees is observed, we propose that the origin of the second transition is the same in both systems. Namely, in freeze concentrated glasses ice starts to melt immediately above T_g', which decreases the glucose concentration and which thus leads to a lower second transition temperature.

This difference between the two systems can be explained quantitatively as follows. The glucose concentration in the freeze concentrated phase at the second transition temperature, T_{tr2} = 230 K, is calculated to be 72 wt % (as obtained from the amplitude of the mobile component (Fig. 4C)). This value for a freeze concentrated system corresponds well to the value of 74 wt % at the crossover temperature of 230 K in a concentrated system (as determined from the line BAC in the state diagram). Hence the second transition temperature in a freeze concentrated glucose systems is equal to the crossover temperature in a concentrated glucose system provided that its glucose concentration equals the concentration of glucose in the freeze concentrated system at this temperature.

Thus the second transition in a concentrated system is similar to the second transition in a freeze concentrated system.

93

In concentrated systems, the occurrence of a crossover temperature has been proposed in a previous section to form the underlying cause of collapse phenomena in concentrated glucose-water glasses. Taking into account our conclusion that the second transition in a concentrated system (i.e. crossover temperature) must be similar to the second transition in a freeze concentrated system, we propose that this second transition in freeze concentrated systems is related to collapse phenomena in these systems. This is observed as an increase in rate of ice melting (Fig. 4 C). Furthermore, the modulus in freeze concentrated glasses obtained in bending tests also decreases in two steps [22, 23].

The state diagram of glucose water mixtures, as shown in Fig. 2, summarizes all results. A maximally freezeconcentrated glucose-water glass (81 wt %) undergoes a glass transition at 220 K, i.e. point D in Fig. 2. Immediately above T_g' ice starts to melt slowly and this corresponds to a steep freezing point depression line (line DA in Fig. 2). At a temperature of 230 K, the line BAC, representing the crossover temperature line, crosses the freezing point depression line at point A. This implies that the molecular mobility in the glucose-water mixture progressively increases. This is accompanied by an increase in the amount of ice melting per degree resulting in a more horizontal freezing point depression line at higher temperatures. Line AD and the literature freezing point depression line (Fig. 2) cannot be smoothly connected because they represent different melting temperatures. The literature freezing point depression line represents the peak temperatures of the melting process observed in the DSC curves [25]. The NMR line represents the ice melting process which starts at a lower temperature (immediately above T_g'). In that case some ice has melted before the DSC melting temperature is reached and the glucose concentration calculated from the NMR results will thus be smaller.

94

This leads to a freezing point depression line at lower temperatures than the DSC freezing point depression line.

CONCLUSION

A second transition in proton mobility is observed, above the glass transition temperature, and is interpreted as the crossover temperature. We propose that this second transition is the origin of collapse phenomena in both concentrated and freeze concentrated sugar glasses, thereby marking their limit of mechanical stability.

ACKNOWLEGDEMENT

REFERENCES

1. Y. Roos *Phase Transitions in Foods*; Academic Press: San Diego, 1995.

2. E. C. To and J. M. Flink. *J. Fd Technol.* **1978**, *13*, 567-581.

3. S. Tsourouflis, J. M. Flink and M. Karel. *J. Sci. Fd. Agric.* **1976**, *27*, 509-519.

4. H. Levine and L. Slade. *Cryo-Lett.* **1988**, *9*, 21-63.

5. A. P. MacKenzie. *Phil. Trans. R. Soc. Lond.* **1977**, *B*, 167-189.

6. E. Y. Shalaev and F. Franks. *J. Chem. Soc. Faraday Trans.* **1995**, *91*, 1511-1517.

7. S. Ablett, A. H. Darke, M. J. Izzard and P. J. Lillford *Studies of the glass transition in malto-oligomers*; Nottingham University Press: Nottingham, 1993.

8. I. J. van den Dries, D. van Dusschoten and M. A. Hemminga. *J. Phys. Chem.* **1998**, *102*, 10483-10489.

9. A. Abragam *The principles of nuclear magnetism*; Clarendon Press: Oxford, 1961.

10. V. J. McBrierty and K. J. Packer *Nuclear magnetic resonance in solid polymers*; Cam. Univ. Press: Cambridge, 1995.

11. S. Ablett, M. J. Izzard and P. J. Lillford. *J. Chem. Soc. Far. Trans.* **1992**, *88*, 789-794.

12. T. R. Noel, R. Parker and S. G. Ring. *Carbohydr. Res.* **1996**, *282*, 193-206.

13. A. P. Sokolov. *Endeavour* **1997**, *21*, 109-113.

14. H. Z. Cummins, G. Li, Y. H. Hwang, G. Q. Shen, W. M. Du, J. Hernandez and N. J. Tao. *Zeitschrift Fur Physik B Condensed Matter* **1997**, *103*, 501-519.

15. W. Schnauss, F. Fujara and H. Sillescu. *J. Chem. Phys.* **1992**, *97*, 1378-1389.

16. E. Rössler, J. Tauchert and P. Eiermann. *Journal of Physical Chemistry* **1994**, *98*, 8173-8180.

17. A. P. Sokolov. *J. Non-Cryst. Solids* **1998**, *235*, 190-195.

18. H. Wagner and R. Richert. *J. Non-Cryst. Solids* **1998**, *242*, 19-24.

19. H. Wagner and R. Richert. *J. Phys. Chem. B* **1999**, *103*, 4071-4077.

20. G. R. Moran and K. R. Jeffrey. *J. Chem. Phys.* **1999**, *110*, 3472-3483.

21. E. Rossler, K. U. Hess and V. N. Novikov. *J. Non-Cryst. Sol.* **1998**, *223*, 207-222.

22. W. M. MacInnes. 2nd year report of the FAIRCT961085 project Molecular Mobility in Foods, 1999.

23. W. M. MacInnes. Dynamical Mechanical Thermal analysis of sucrose solutions. In *The glassy state in foods*; J. M. V. Blanshard and P. J. Lillford, Eds.; Nottingham University Press: Nottingham, 1993; pp 223-248.

24. Y. Roos and M. Karel. *Int. J. Food Sc. Tech.* **1991**, *26*, 553-566.

25. B. Luyet and D. Rasmussen. *Biodynamica* **1968**, *10*, 167-191.

26. F. E. Young. *J. Phys. Chem.* **1957**, *61*, 616.

SUMMARY

Glasses are liquids that exhibit solid state behavior as a result of their extremely high viscosity. Regarding their application to foods, glasses play a role in the preservation of foods, due to their high viscosity and the concomitant low molecular mobility. This thesis focuses on sugar glasses. Sugar glasses are relevant as model systems for foods that contain sugars and have a low water content and/or that are frozen, since in both types the sugars can exist in the glassy state. Often, the stability of these types of foods can be attributed to the stability of the sugar glasses. Key factors controlling the stability are e.g. water content and temperature.

The work presented in this thesis aims at relating the stability of sugar glasses to molecular mobility, as a function of water content and temperature. More specifically, molecular mobility in sugar-water glasses was studied using two magnetic resonance techniques and subsequently related that to stability data obtained from the literature. Using the first technique, i.e. saturation transfer electron spin resonance (ST-ESR), the rotational mobility of a spin probe, added to the sugar-water mixture, was obtained. Using the second technique, a proton magnetic resonance (^{1}H-NMR) technique, the relaxation behavior of the protons was determined. This is a measure of rotational proton mobility of both sugar and water molecules.

After the general introduction in chapter 1, a new data analysis of the ST-ESR spectra is proposed in chapter 2. This analysis has been developed to extend the range of rotational correlation times (τ_R) up to values around 10^{+4} s. This is necessary to obtain the τ_R values of very slow rotating spin probes, as present in a glassy material. The new data analysis of the saturation transfer ESR spectra is based on the diffusion as well as the recovery of saturation in

competition with the field modulation. The previous data analysis was based on taking into account only the influence of diffusion on the spectra and, since the spectra are not sensitive for rotational diffusion with values of $\tau_R > 10^{-3}$ s, this was the limiting τ_R value. The new data analysis takes into account that the spectra are sensitive for the recovery process (T_1). This recovery process is linearly correlated with τ_R. In this way, the new analysis of saturation transfer ESR data provides values for very slow rotational mobilities up to τ_R values of around 10^{+4} s.

Chapter 3 describes the use of the ^{1}H-NMR technique to obtain molecular mobility of the water and sugar protons as a function of water content and temperature, in maltose-water glasses. In the ^{1}H-NMR signal, slow decaying and fast decaying fractions of protons are distinguished, arising from mobile and immobile ($\tau_R > 3*10^{-6}$) protons, respectively. The assignment of mobile and immobile proton fractions to water and maltose protons is temperature dependent. Roughly however, water protons can be considered as mobile (except below T_g) and maltose protons as immobile (becoming mobile above T_g). By analyzing the relaxation behavior of the mobile protons, the mobility of the water molecules was determined. The method of second moments yielded information on the anisotropic mobility as well as proton density of the immobile protons. The mobility of both water and sugar protons were found to increase with temperature. The glass transition is found to be characterized by a continuous increase in mobility. Upon increasing water content, both sugar and water molecules are found to become more mobile.

In Chapter 4, both magnetic resonance techniques are applied to various sugar-water glasses with varying water content, as a function of temperature. In order to compare the mobility in different glasses, T_g was taken as the reference point. By increasing the water content from 10 to 30 wt %, the spin

probe mobility at T_g was found to decrease, while the water mobility at T_g was found to increase. This apparent paradox is explained on the basis of our experimental findings as follows. If water is added to a sugar glass, the average distance between the sugar molecules increases, leading to an increase in water mobility at T_g. However the overall packing of water and sugar becomes denser at first, with increasing water content as deduced from Fourier transform infrared spectroscopy experiments. Thus the spin probe is hindered more in its rotation, leading to decreasing spin probe mobility at T_g. The increasing amount of water yields on the other hand a larger mobility of the water molecules. We note that this effect of molecular packing is also exemplified by comparing the effects of carbohydrate molecules with increasing molecular weight (ranging from glucose up to maltoheptaose), while keeping the water content constant. Both water and spin probe mobility at T_g increase upon increasing the molecular weight of the malto-oligomer. This can be explained by the fact that larger oligomers form less densely packed networks resulting in an increasing spin probe and water mobility.

Chapter 5 focuses on a second transition in mobility of the sugar protons. In concentrated glucose glasses this second transition occurs about 20 to 30 degrees above the glass transition temperature. Its dependence on water content is shown as a new line in the state diagram of glucose-water mixtures. In freeze concentrated glucose glasses a similar second transition is found. The second transition is interpreted as the so-called crossover temperature, where the dynamics changes from solid like to liquid like. In freeze concentrated glasses an increase in the amount of ice melting per degree is observed just above the temperature of the second transition. It is proposed that both in concentrated and freeze concentrated glucose glasses, this second transition relates to so-called collapse phenomena in sugar-water mixtures.

In Chapters 4 and 5, two different aspects of stability of sugar glasses have been related to molecular mobility. The long-term storage stability relates to molecular mobility *in* the glassy state (Chapter 4). It is shown how sugar, water and spin probe mobility in the glassy state depends on water content and type of sugar. The short-term stability, e.g. important during processing, relates to molecular mobility at the collapse temperature, i.e. ±20 degrees above T_g. In Chapter 5, it is concluded that the origin of collapse phenomena signifies an abrupt increase in molecular mobility of the sugar protons at the collapse temperature. In conclusion, effects of water, temperature and type of sugar on molecular mobility have been established and related to aspects of stability of sugar glasses.

SAMENVATTING

Glazen zijn vloeistoffen die zich gedragen als vaste stoffen omdat ze een extreem hoge viscositeit hebben. In voedsel spelen glazen een rol in de conservering van voedsel dankzij hun hoge viscositeit en de bijbehorende lage moleculaire beweeglijkheid. Dit proefschrift gaat over suikerglazen. Deze glazen zijn relevant als model systemen voor voedsel met een laag watergehalte en bevroren voedsel omdat in beide types voedsel de suikers in glastoestand voorkomen. Vaak wordt de stabiliteit van dit soort voedsel bepaald door de stabiliteit van het suikerglas. Belangrijke factoren die de stabiliteit beïnvloeden zijn bijvoorbeeld watergehalte en temperatuur.

Het onderzoek in dit proefschrift heeft als doel om de stabiliteit van suikerglazen te relateren aan moleculaire beweeglijkheid als een functie van watergehalte en temperatuur. Moleculaire beweeglijkheid in suiker-water glazen is bestudeerd met twee magnetische resonantie technieken en vervolgens gerelateerd aan stabiliteitdata uit de literatuur. Met de eerste techniek, saturation transfer electron spin resonance (ST-ESR), wordt de rotatie beweeglijkheid van een spin probe, die is toegevoegd aan het suiker-water mengsel, gemeten. Met de tweede techniek, een proton magnetische resonantie (^{1}H-NMR) techniek, wordt het relaxatiegedrag van protonen bepaald. Dit is een maat voor de rotatie beweeglijkheid van de suiker en water protonen.

Na de algemene introductie in hoofdstuk 1, wordt in hoofdstuk 2 een nieuwe data analyse methode geïntroduceerd. Omdat in glazen heel langzaam roterende spin probes aanwezig zijn is het nodig om d.m.v. een nieuwe data analyse het bereik van rotatie correlatie tijden (τ_R) uit te breiden tot 10^{+4} s. Saturation transfer ESR is erop gebaseerd dat de verzadiging wordt opgeheven

101

door zowel diffusie als ook relaxatie in competitie met de veldmodulatie. De standaard data analyse houdt alleen rekening met de invloed van diffusie op de spectra. De spectra zijn gevoelig voor rotatie diffusie met τ_R waardes tot 10^{-3} s en dat is daarom de limiet waarde die bepaald kan worden. De nieuwe data analyse verdisconteert ook de invloed van relaxatie op de spectra. Dit relaxatieproces is lineair gecorreleerd met τ_R. Op deze manier kunnen τ_R waardes van heel langzaam roterende spin probes worden bepaald met een limiet waarde van $\tau_R \sim 10^{+4}$ s.

Hoofdstuk 3 behandelt het gebruik van een ^{1}H-NMR techniek om de moleculaire beweeglijkheid van water en suikerprotonen te meten als functie van watergehalte en temperatuur in maltose-water glazen. In het ^{1}H-NMR signaal kunnen twee fracties worden onderscheiden die snel en langzaam relaxeren en respectievelijk afkomstig zijn van immobiele ($\tau_R > 3 * 10^{-6}$ s) en mobiele protonen. De toekenning van mobiele en immobiele protonen aan suiker en water protonen is temperatuurafhankelijk. Ruwweg zijn de water protonen mobiel (behalve beneden T_g) en de maltose protonen immobiel (en worden mobiel boven T_g). Door het relaxatiegedrag van de mobiele protonen te analyseren kan de beweeglijkheid van de waterprotonen worden bepaald. De methode van het tweede moment levert informatie over de beweeglijkheid en protonendichtheid van de immobiele protonen. De beweeglijkheid van zowel water als suikerprotonen neemt toe met de temperatuur. De glasovergang wordt gekarakteriseerd door een toename in beweeglijkheid. Met toenemend watergehalte neem de beweeglijkheid van zowel water als suiker moleculen toe.

In hoofdstuk 4 zijn beide magnetische resonantie technieken toegepast op verschillende suiker-water glazen met variërend watergehalte als functie van de temperatuur. Om de beweeglijkheid in verschillende glazen te kunnen

verglijken is T_g als referentie temperatuur genomen. Als het watergehalte van 10 naar 30 wt% gaat, neemt de spin probe beweeglijkheid op T_g af terwijl de waterbeweeglijkheid op T_g toeneemt. Deze ogenschijnlijke paradox wordt als volgt uitgelegd. Als water wordt toegevoegd aan het suikerglas neemt de gemiddelde afstand tussen de suikermoleculen toe en daardoor heeft het water meer ruimte om te bewegen, leidend tot een toename in de waterbeweeglijkheid. Maar de pakkingdichtheid van het hele systeem (water + suiker) neemt toe, zoals blijkt uit Fourier transform infrared spectroscopy experimenten. Dus de spin probe wordt meer gehinderd bij het roteren wat leidt tot een afnemende spin probe beweeglijkheid op T_g. Het moleculaire pakkingargument verduidelijkt ook de effecten die optreden bij toenemend molecuulgewicht van het suiker (van glucose tot maltoheptaose). Zowel spin probe als waterbeweeglijkheid op T_g neemt toe met toenemend molecuulgewicht omdat grotere oligomeren minder dicht pakken dan kleinere wat resulteert n een toenemende water en spin probe beweeglijkheid.

Hoofstuk 5 focust op een tweede overgang in beweeglijkheid van de suikermoleculen. In geconcentreerde glucose glazen ligt deze overgang 20-30 graden boven de glasovergang. Een nieuwe lijn in het toestandsdiagram van glucose-water geeft de afhankelijkheid van de tweede overgang van watergehalte. In gevriesconcentreerde glucoseglazen treedt een soortgelijke overgang op. De tweede overgang interpreteren we als de crossover temperatuur, waar de dynamica verandert van vaste stof-achtig naar vloeistof-achtig. In gevriesconcentreerde glazen gaat de tweede overgang gepaard met een toename in de ijssmeltsnelheid. Ook in geconcentreerde glucose glazen gaat de tweede overgang gepaard met collapse verschijnselen.

In hoofdstuk 4 en 5 zijn twee verschillende aspecten van stabiliteit van suikerglazen gerelateerd aan moleculaire beweeglijkheid. De lange termijn

opslag stabiliteit is gerelateerd aan moleculair beweeglijkheid *in* het glas (hoofdstuk 4). We laten zien hoe suiker, water en spin probe beweeglijkheid in de glastoestand afhangen van watergehalte en type suiker. De korte termijn stabiliteit bijvoorbeeld belangrijk tijdens verwerking van suiker-water mengsels, is gerelateerd aan moleculaire beweeglijkheid op de collapse temperatuur, dat is 20-30 graden boven T_g. Uit de resultaten van hoofdstuk 5 concluderen we dat collapse verschijnselen gepaard gaan met een abrupte toename in beweeglijkheid van de suikerprotonen op de collapse temperatuur. Kortom, effecten van water, temperatuur en type suiker op moleculaire beweeglijkheid zijn gemeten en gerelateerd aan aspecten van stabiliteit van suikerglazen.

NAWOORD

Zo dat zit er weer op, tijd voor iets anders. Maar niet zonder de mensen te bedanken die een bijdrage hebben geleverd. Allereerst Erik wiens enthousiasme op het juiste moment kwam. Hoewel ik nooit zo precies en nauwkeurig zal schrijven als jij heb ik er veel van geleerd. Marcus, bedankt voor de begeleiding en deelname aan het molecular mobility in foods project. Dat schiep de mogelijkheid om te praten met mensen die met soortgelijk onderzoek bezig waren, precies wat ik graag doe. Verder wil ik iedereen op Moleculaire Fysica bedanken, voor de koffie op het lab, voor technische of computer hulp, voor een eigengereide intro op de NMR en het uitblazen in de kroeg. Hoewel ik als student riep dat ik nooit bij die nurds op Moleculaire Fysica zou willen werken, bleek het heel gezellig. In eerste instantie werd het gebrek aan labuitjes naadloos opgevangen door Geïntegreerde Levensmiddelentechnologie en Fysica, wat een mooi moment was om jullie te leren kennen. Hoewel ik slechts zelden in het Biotechnion kwam heb me altijd welkom gevoeld, daarvoor bedankt. Ook Mark leverde op geheel eigen wijze een bijdrage aan dit proefschrift door mij aan te sporen ook in het weekend te gaan werken. Dan ging jij wel gezellig mee internetten.

Bedankt,

Ivon

CURRICULUM VITAE

Ivonne Jeanne van den Dries werd geboren op 21 december 1970 in Eindhoven. Na het behalen van haar Gymnasium B diploma aan het Jansenius Lyceum te Hulst, begon zij in 1989 met de studie Moleculaire Wetenschappen aan de Landbouwuniversiteit Wageningen. Deze studie werd afgerond met afstudeervakken bij de vakgroep Fysische en Kolloïdchemie en bij de vakgroep Agrotechniek en Fysica en een stage Organische Chemie aan de Universiteit van Lund (Zweden). Vanaf 1994 was zij werkzaam als Assistent in Opleiding bij de leerstoelgroep Levensmiddelennatuurkunde van de Landbouwuniversiteit Wageningen en verrichte zij onderzoek dat leidde tot dit proefschrift.